EFFECTS OF HORMONE REPLACEMENT THERAPY ON SYSTEMIC ARTERIAL PROPERTIES IN POST-MENOPAUSAL WOMEN

by

Eric Alps Chen

B.S., The Johns Hopkins University, 2000

Submitted to the Graduate Faculty of the

University of Pittsburgh in partial fulfillment

of the requirements for the degree of

Master of Science

in

Bioengineering

University of Pittsburgh

2002

UNIVERSITY OF PITTSBURGH

SCHOOL OF ENGINEERING

This thesis was presented

by

Eric Alps Chen, B.S.

It was defended on

August 14, 2002

and approved by

Harvey S. Borovetz, Ph.D.

Kirk P. Conrad, M.D.

Sanjeev G. Shroff, Ph.D.
Advisor

ABSTRACT

EFFECTS OF HORMONE REPLACEMENT THERAPY ON SYSTEMIC ARTERIAL PROPERTIES IN POST-MENOPAUSAL WOMEN

Eric Alps Chen, B.S.

University of Pittsburgh, 2002

Vascular stiffness properties contribute significantly to the arterial system hydraulic load. There is evidence that vascular stiffness plays a role in cardiovascular remodeling and may be an independent cardiovascular risk factor. Menopause accelerates age-associated increase in arterial stiffness and estrogen administration, which has vasodilating properties, can potentially mitigate this post-menopausal increase in stiffness.

The present study examined the effects of chronic hormone replacement therapy (HRT) on systemic arterial mechanical properties in 35 post-menopausal women, divided into two groups: those receiving no HRT (Control, n = 25) and those receiving HRT (HRT-all, n = 10). The HRT-all group consisted of two subgroups: estrogen alone (HRT-E, n = 5) and a combination of estrogen and progesterone (HRT-EP, n = 5). Noninvasive data were collected serially at five times: once at the baseline during the first visit and during four subsequent visits after the initiation of the study at 19±1, 108±5, 193±4, and

388±8 days, respectively. Heart rate (*HR*), stroke volume (*SV*), and cardiac output (*CO*) did not change significantly in the control group throughout the study. This was also true for both HRT groups, except for a small decrease in *HR* at Visits 3 and 4 for the HRT-E group and an increase in *CO* at Visit 3 in the HRT-EP group. Mean arterial pressure decreased over time in control and both HRT groups, reaching statistical significance at later times (fifth visit). Systemic vascular resistance (*SVR*) did not change significantly in control and both HRT groups. Global arterial compliance (*AC*) was unchanged for the control group but tended to increase in the HRT-all group, although no statistical significance was reached. In contrast, the subgroup analysis revealed that *AC* increased for the HRT-E subgroup, reaching statistical significance at the fifth visit. Similarly, significant decrements in pulse wave velocity (*PWV*), an index of regional vascular stiffness, were observed only for the HRT-E group.

In conclusion, *AC* increased (vascular stiffness decreased) in subjects receiving chronic estrogen therapy only. The inclusion of progesterone seems to counteract the estrogen-mediated decrease in vascular stiffness, indicating that the vascular stiffness-associated cardio-protective effects of HRT, if any, may be limited to estrogen administration alone.

DESCRIPTORS

Cardiovascular Risks	Estrogen
Global Arterial Compliance	Hemodynamics
Hormone Replacement Therapy	Post-menopausal Women
Progesterone	Pulse Wave Velocity
Systemic Vascular Resistance	Vascular Stiffness

ACKNOWLEDGEMENTS

I would like to thank my Master's thesis committee members, Drs. Sanjeev Shroff, Kirk Conrad, and Harvey Borovetz for their valuable guidance and support and their time and effort in reading my thesis. I especially want to thank Dr. Sanjeev Shroff for allowing me to be his student and for his tutelage that he has given me.

Special thanks go to the Echocardiography Laboratory, University of Chicago personnel, especially, Dr. Claudia Korcarz, Dr. Genevieve Giradet-Nendaz, Ms. Lynn Weinert, and Dr. Roberto Lang. All of the noninvasive data acquisition was performed at this laboratory.

I am also appreciative of everyone in the Cardiovascular Systems Laboratory members for their help and encouragement. Specifically, I am grateful to Caroline Czapko for having to listen to me whenever things didn't work out in the lab. Thanks to Roman Tkachev for helping me with data analysis. Many thanks to all my friends that I have made during my time here at the University of Pittsburgh, Jonathan Vandegeest, Thomas Payne, Philip Marascalco, and Thanh Lam.

I would like to thank my family for their love and support ever since I was a little kid and for shaping me to what I am today and to my girlfriend, Quyen, because without you, I would not have been able to do any of this.

Finally, I would like to acknowledge the financial support from NIH grants (R01-AG13920 and R01-HL/HD67937) and the support of the Department of Bioengineering, University of Pittsburgh.

TABLE OF CONTENTS

LIST OF TABLES

LIST OF FIGURES

NOMENCLATURE

Acronyms & Symbols

AC	global arterial compliance
A_d	area underneath the diastolic portion of the carotid (aortic) pressure waveform
CO	cardiac output
D_{LVOT}	left ventricular outflow tract diameter
HR	heart rate
HRT	hormone replacement therapy
HRT-all	group consisting of all subjects receiving hormone replacement therapy
HRT-E	group consisting of subjects receiving estrogen alone (a subset of HRT-all)
HRT-EP	group consisting of subjects receiving estrogen and progesterone (a subset of HRT-all)
MAP	mean arterial pressure
P_d	arterial minimum diastolic pressure
$P_{s\text{-}carotid}$	carotid peak systolic pressure
$P_{s\text{-}brachial}$	brachial peak systolic pressure
$PWV_{C\text{-}F}$	carotid-to-femoral pulse wave velocity
$PWV_{B\text{-}R}$	brachial-to-radial pulse wave velocity

P_1	carotid peak pressure point following the dicrotic notch
P_2	carotid minimum diastolic pressure point (same as P_d)
RI	global reflection index
SV	stroke volume
SVR	systemic vascular resistance
t_d	duration of diastole
W_{tot}	total power
W_{std}	steady power
W_{osc}	oscillatory power
$\%W_{osc}$	percent oscillatory power
Z_c	carotid (aortic) characteristic impedance
Z_{in}	carotid (aortic) input impedance spectrum
Z_1	modulus of first (fundamental) harmonic of the input impedance spectrum
$\|\Gamma_1\|$	magnitude of the first harmonic of global reflection coefficient spectrum

1.0 INTRODUCTION

Hardening of the pulse, first described thousands of years ago by Chinese healers, was known even then to be an adverse prognostic sign[1]. In Western civilization, the changes in arterial stiffness with normal aging and certain pathological conditions (e.g., hypertension, arteriosclerosis) have been documented for some time now[2]. Arterial stiffness is being recognized as a risk marker for coronary heart disease and is potentially modifiable[2]. Epidemiological studies have shown that the incidence of cardiovascular disease and risks are lower in pre-menopausal women compared to similar-aged men, and these gender differences seem to disappear in the post-menopausal state[3]. In some of the previous studies, there is evidence indicating that hormone replacement therapy (HRT) for post-menopausal women, which includes estrogen, significantly decreases cardiovascular disease and risks[4,5]. The goal of the present study was to examine the long-term effects of HRT on systemic arterial mechanical properties in post-menopausal women.

Note: All numerical references can be found in the bibliography.

2.0 BACKGROUND

2.1 Basic Principles of Systemic Arterial Function

As discovered by the British physiologist William Harvey in 1628, the cardiovascular system contains two circuits: systemic and pulmonary circulations. Deoxygenated blood from the right ventricle is pumped through the pulmonary arterial circulation, oxygenated in the lungs, and returned to the left atrium. Oxygenated blood is then pumped from the left ventricle into all organs and tissues (systemic arterial circulation) and then returns via the systemic venous circulation to the right atrium. The present work focuses on the systemic arterial circulation, which begins with a single vessel originating from the left ventricle (ascending aorta) and subsequently divides into gradually smaller arteries. These arteries ultimately branch into arterioles and then further into smaller vessels, capillaries.

The basic functional and structural characteristics of systemic arteries change as they go from the aorta down to the capillaries. All systemic arterial vessels are comprised of endothelial cells, smooth muscle, and connective tissue (e.g., elastin and collagenous fibers), except for capillaries that are primarily made up of endothelial cells. Endothelial cells form the inner lining of the vessels and possess a number of functions that play an important role in modulating arterial mechanical properties. The level of smooth muscle activation and arterial vessel remodeling (i.e., vascular geometry, vessel wall mass, and relative amounts of elastin, collagen, and smooth muscle) also affect arterial mechanical properties.

From the functional viewpoint, most of the hydraulic resistance to blood flow is provided by arterioles, which contain smooth muscle and have the ability to vasodilate (an increase in radius) or vasoconstrict (a decrease in radius). It is clear that a number of substances can cause contraction or relaxation of vascular smooth muscle[6]. Many of these substances act directly on the smooth muscle, but some of them act on the endothelial cells nearby the smooth muscle. These endothelial cells respond to these substances by releasing paracrine agents that diffuse to the neighboring smooth muscle and cause vasodilation or vasoconstriction.

In order to meet the continuous needs of peripheral tissues for oxygen and substrate delivery, the arterial tree must convert cardiac pulsations into a more constant flow pattern in the distal circulation[1]. This conversion of pulsations occurs in the proximal vessels (aorta and large arteries) during systole. These proximal vessels have thick walls containing a significant quantity of elastic tissue. Due to the large radii of the arteries, they serve as low resistance, elastic tubes. A portion of the cardiac stroke volume remains in the arteries during systole and the subsequent elastic recoil pushes the remaining blood to the periphery during diastole, resulting in a near-steady end-organ perfusion. Blood vessels that have a high compliance value or low stiffness experience only small change in systolic pressure for a given change in volume. Therefore, people with compliant vessels have low pulse pressures while the opposite is true for stiff vessels. In brief, vascular compliance (stiffness) properties govern pressure and flow pulsatilites in the systemic arterial circulation.

2.2 Quantitative Characterization of Arterial Mechanical Properties

2.2.1 Input Impedance Spectrum

The arterial system hydraulic load is the opposition to movement of blood out of the ventricle. Systemic arterial input impedance spectrum (Z_{in}) is a comprehensive and quantitative characterization of this hydraulic load[7-12]. A typical example of aortic Z_{in} in the human setting, calculated as the harmonic ratio of aortic pressure (P_{ao}) to flow (Q_{ao}), is shown in Figure 1.

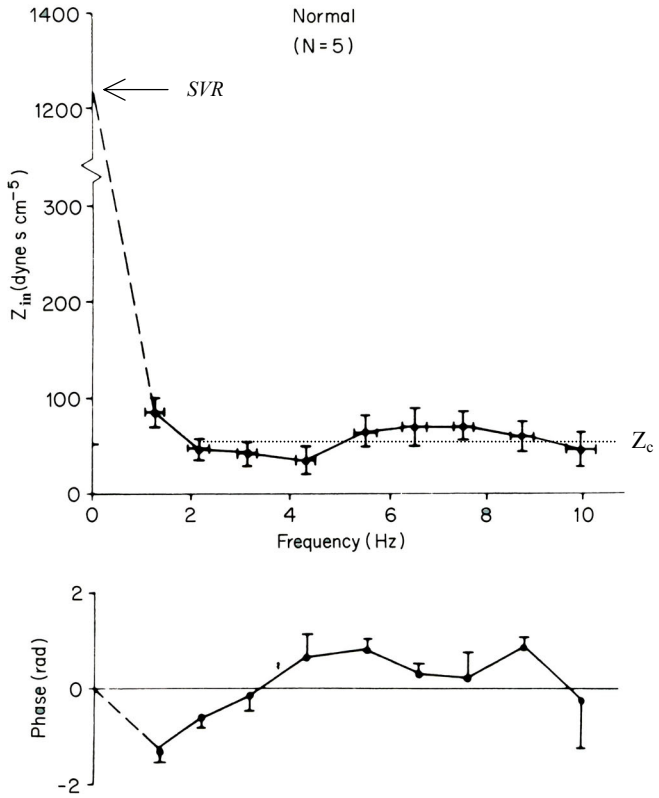

Figure 1: Aortic input impedance spectrum, adapted from Nichols *et al*. (1977)

Z_{in} is a frequency-dependent quantity and is made up of two components, magnitude and phase, which describe the magnitude of hydraulic load and the phase shift at each frequency, respectively. The magnitude of Z_{in} begins with a high value at zero frequency. It falls as frequency increases and oscillates before reaching a constant value at high frequencies. The overall compliance of the arterial circulation is one of the determinants of the rate of fall of Z_{in} magnitude. The phase angle is zero at zero frequency, negative at low frequencies, and makes a transition to positive values before returning back to zero at high frequencies.

Although Z_{in} is a comprehensive characterization of arterial mechanical properties, it is relatively an abstract concept and a relationship, i.e., a function of frequency. Therefore, arterial hydraulic load is usually separated into two components: a steady component and a pulsatile component.

2.2.2 Steady Component of Systemic Arterial Load

The steady component of systemic arterial load, commonly termed as systemic vascular resistance (*SVR*.), is identical to the magnitude of Z_{in} at zero frequency. As discussed before, *SVR* is the hydraulic resistance to mean blood flow, residing primarily in the arterioles. This quantity is relatively easy to obtain (mean aortic pressure/mean aortic flow) and can be physically interpreted. It is typically the only parameter used in the clinical setting to quantify arterial load.

2.2.3 Pulsatile Component of Systemic Arterial Load

Pulsatile load originates from the geometric and elastic properties of the vessels and the fluid properties of the blood flowing through it. Unlike the steady load, pulsatile load cannot be quantified in terms of a single number. For example, the information about the pulsatile component is located in the non-zero frequency components of Z_{in}. As mentioned above, quantitation in terms of Z_{in} is very abstract and therefore, indices have been developed to characterize various aspects of pulsatile load (e.g., global arterial compliance, characteristic impedance, pulse wave velocity, wave reflection).

2.2.3.1 Global Arterial Compliance

Static vascular compliance is the steady-state change in vascular volume for a given change in pressure, i.e., the slope of vascular pressure/volume relationship[13]. Such steady-state measurements are not possible under *in vivo* conditions and therefore, indices of arterial compliance are derived from simultaneous measurements of aortic pressure and flow data. Global arterial compliance (*AC*) is one such index that is estimated either from the diastolic aortic pressure decay[14] or by fitting instantaneous pressure and flow over the entire cardiac cycle[15]. *AC* is a property of the entire systemic arterial circulation and is determined by elastic, geometric, and architectural (i.e., branching pattern) properties of systemic circulation. As systemic arteries get less stiff, *AC* is expected to increase and *vice a versa.*

2.2.3.2 Characteristic Impedance

As discussed before, the magnitude of Z_{in} levels off at high frequencies; and this value is defined as the characteristic impedance (Z_c). Unlike *AC*, Z_c is a local characterization and is determined by the geometric and elastic properties of the site at which pressure and flow are measured. For an uniform cylindrical tube with purely elastic wall and nonviscous fluid with only axial flow, Z_c is given by: (ρ indicates blood density; E_{inc}, elastic modulus; h, thickness; R_i, vessel internal radius)[11]:

$$Z_c = \sqrt{\frac{\rho}{3\pi^2}\frac{E_{inc}h(2R_i+h)}{R_i^4(R_i+h)^2}}\,. \tag{2-1}$$

Z_c varies directly with the elastic modulus of the artery (i.e., stiffness) and inversely related to its lumen size. If Z_{in} is calculated from the measurements of ascending aortic pressure and flow then Z_{in} is a characterization of the entire systemic arterial circulation and Z_c is the characterization of the site of measurement (i.e., ascending aorta).

2.2.3.3 Pulse Wave Velocity

Pulse wave velocity (*PWV*) is the speed with which pressure or flow waves travel along an arterial segment. Similar to Z_c, *PWV* is a local characterization in that it is a property of the vessel segment in question. Physically, the elastic and geometric (lumen diameter and wall thickness) properties of the vessel segment determine *PWV*. For an uniform elastic cylindrical tube with purely elastic wall and nonviscous fluid with only

axial flow, *PWV* is given by: (ρ indicates blood density; E_{inc}, elastic modulus; h, thickness; R_i, vessel internal radius)[11]:

$$PWV = \sqrt{\frac{1}{3\rho}\frac{E_{inc}h(2R_i + h)}{(R_i + h)^2}}. \qquad (2\text{-}2)$$

As a consequence of increasing vessel wall stiffness and decreasing caliber, *PWV* increases as one moves from the heart to the peripheral circulation (Figure 2).

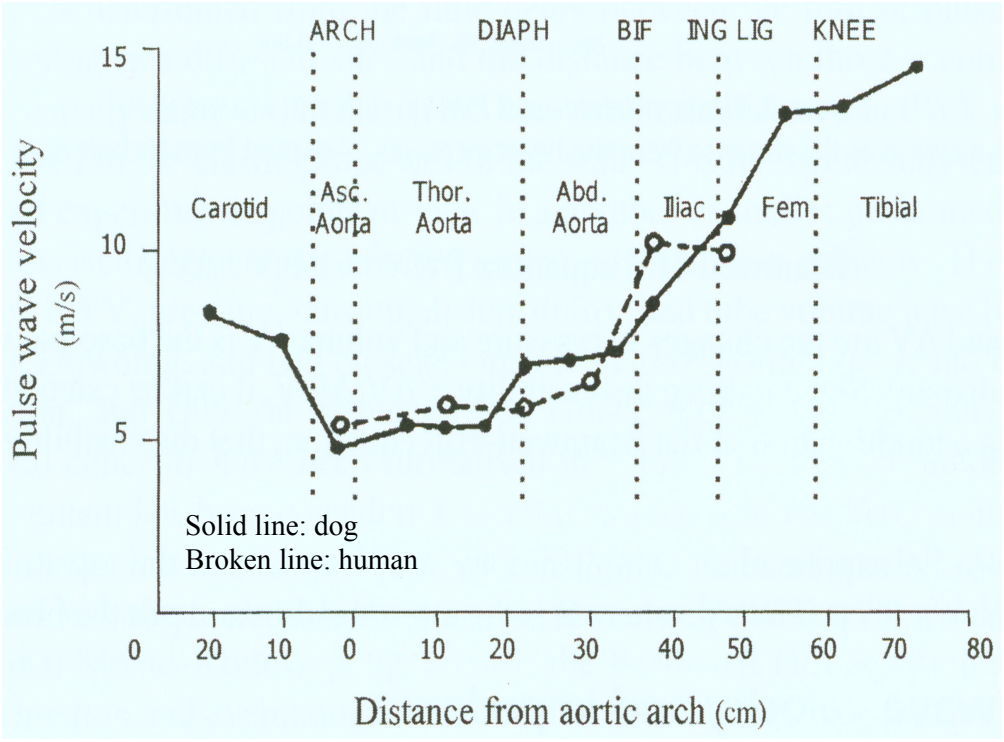

Figure 2: Regional differences in pulse wave velocity (adapted from Asmar R., 1999)

PWV of a given region has been found to increase with aging, hypertension, and renal failure[2,16] and also has been useful in determining the vascular effects of vasodilating drugs and antihypertensive therapies[17].

2.2.3.4 Wave Reflection Indices

The pulsatile ejection of blood from the left ventricle results in a pressure wave (which is an acoustic wave) that travels towards the peripheral circulation. Throughout the cardiovascular system, there are many sites where impedance mismatch occurs (e.g., arterial branching points and terminations at the arteriolar level). At these sites, a fraction of the pressure wave is reflected back towards the heart. The body size of the person, location of the heart along the long axis, and *PWV* determine the timing of these reflected waves at the ascending aorta, while the magnitude of the reflected wave is dependent on the magnitude of the impedance mismatch.

Several quantitative characterizations of overall arterial wave reflection have been developed. For example, global reflection coefficient, Γ, is defined as:

$$\Gamma = \frac{\left(Z_{\text{in}} - Z_{\text{c}}\right)}{\left(Z_{\text{in}} + Z_{\text{c}}\right)}. \tag{2-3}$$

Because Z_{in} is a complex number and a function of frequency, Γ is also a complex quantity that varies with frequency. The magnitude of Γ ($|\Gamma|$) lies between 0 (no reflections) and 1 (maximum reflections) and one typically focuses on its first harmonic, $|\Gamma_1|$. Another approach for quantifying arterial wave reflections is to first decompose aortic pressure and flow waves into forward (i.e., traveling away from the heart) and backward (i.e., traveling towards the heart) waves[18] and then calculate reflection index (*RI*) as the ratio of forward and backward pressure (or flow) wave amplitudes. Wave reflections can significantly alter aortic pressure wave morphology. For example, differences in aortic pressures between old and young subjects are illustrated in Figure 3.

In the old subject, the peak of the reflected wave occurs during systole such that there is a secondary rise in systolic pressure. This early return of the reflected wave is due to the increased *PWV* known to occur with aging (increased vascular stiffness). The secondary rise in systolic pressure imposes an additional load on ventricular ejection and is likely to increase myocardial oxygen consumption. In the younger subject, the reflected wave occurs during diastole causing an augmentation of aortic pressure during diastole. This diastolic pressure augmentation is likely to be beneficial from the perspective of cardiac perfusion.

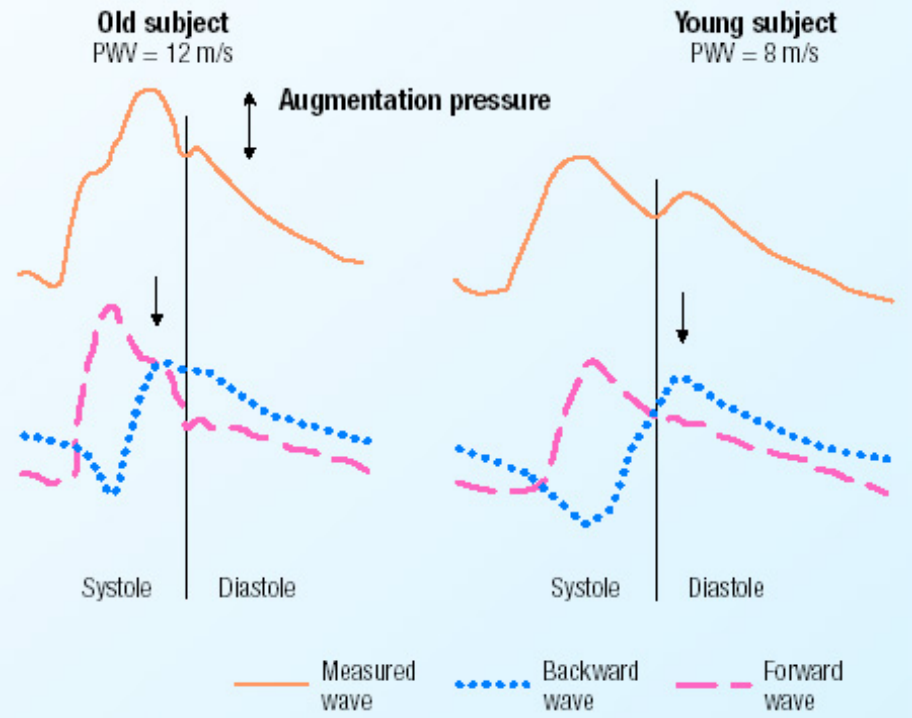

Figure 3: Central pressure contours (from Asmar R., 1999)

2.3 Pulsatile Arterial Load and Cardiovascular Remodeling and Risk

Acute changes in pulsatile arterial load primarily affect pressure and flow wave morphologies[10,18-21]; the effects on mean pressure and flow, however, are small. For example, an increase in vascular wall stiffness, a quantity that is inversely proportional to global arterial compliance, with all other factors held constant, shows a significant increase in pressure and flow pulsatilities, e.g., a greater pulse pressure with a taller and narrower flow pulse. It is commonly accepted that the greater pulse pressure is related to an increased systolic aortic pressure, however our studies[21] have shown that changes in diastolic aortic pressures have greater contribution to the changes in pulse pressure.

The mean blood pressure, determined by *SVR* and cardiac output, is a major determinant of left ventricular (LV) hypertrophy[22,23]. The role of pulsatile arterial load in this remodeling process may be more important than previously acknowledged. From a vascular perspective, increased pulse pressure or cyclic wall stress (strain) has been postulated to accelerate the normal age related remodeling of the arterial wall (vessel dilation and stiffening of the wall)[24,25]. In addition to its effects on cyclic wall stress (strain), increased flow pulsatilities result in an increase in oscillatory shear stress at the vascular endothelium. It is known that endothelial shear stress is a modulator of endothelial function and of vascular mechanical behavior.

Several epidemiological studies have shown that both diastolic and systolic blood pressures and the presence of LV hypertrophy are independent risk factors for cardiovascular diseases[26-32]. A study by Darne *et al*.[33] describes the relationship between steady and pulsatile component indices of blood pressure and cardiovascular mortality.

Their longitudinal study indicated that the steady component index was a strong predicting factor in both males and females for all types of cardiovascular diseases, however the pulsatile component index in women over the age of 55 years was linked to mortality from coronary artery disease.

2.4 Post-menopausal Women

Menopause is the irreversible end of the reproductive stage in a woman's life. This usually occurs around the age of 50 with menstrual cycles becoming less frequent. Menopause is caused primarily by ovarian failure when the ovaries fail to respond to the gonadotropins (sex hormones) mainly because the follicles and eggs have disappeared through atresia[6]. Although small amounts of estrogen are still secreted into the plasma, largely from the alteration of adrenal androgens to estrogen, menopause is associated with a precipitous fall in plasma estrogen levels. Menopause is associated with osteoporosis (decrease in boss mass and strength), hot flashes, night sweats, vaginal dryness, and increase in cardiovascular disease.

Epidemiological studies have shown that the incidence of cardiovascular disease and risks are lower in pre-menopausal women compared to similar-aged men and these gender differences disappear in the post-menopausal state[3] (Figure 4). Studies have shown that women have higher levels of triglycerides, cholesterol, and, low-density lipoprotein cholesterol after menopause as compared to pre-menopausal women[34]. These changes are due to a combination of the following factors: the effects of menopause (decrease in estrogen hormone production), weight gain, and aging. Menopause can be

caused surgically. In this case the risks of cardiovascular disease seem to increase much more rapidly than those seen with natural menopause.

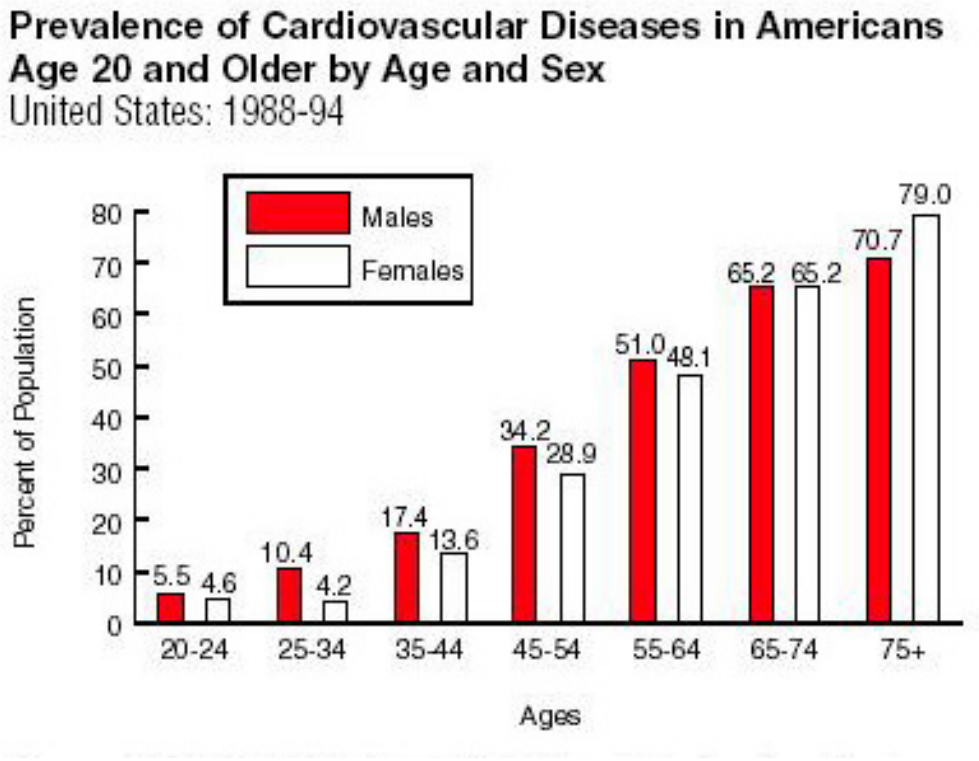

Figure 4: Prevalence of cardiovascular diseases (from AHA 2002, www.americanheart.org)

2.5 Hormone Replacement Therapy

Increasing plasma estrogen level by administering exogenous estrogen was the primary focus of the original hormone replacement therapy (HRT). Although this form of HRT is effective in preventing menopause-associated osteoporosis and hot flashes, the long-term usage increases the risk of developing uterine endometrial cancer[6]. It was found that the increased risk of endometrial cancer is virtually absent when progesterone

is added along with estrogen. Thus, the current form of HRT consists of administering estrogen and progesterone, except for those women who have had a hysterectomy; here estrogen alone can be taken.

Several studies indicate that there is a decrease of cardiovascular disease in women with post-menopausal HRT and increase in survival rates of women with coronary artery disease[35]. It was argued that HRT significantly decreases mortality in post-menopausal women, principally through the cardio-protective ability of estrogen against heart disease[6]. However, the most recent study[36] indicates that HRT is actually associated with increased risk of coronary heart disease (CHD) during the first year, and a decreased risk during years 3 to 5. This was a randomized, double blinded, placebo-controlled trial of 4.1 years' duration (HERS) and subsequent unblinded follow-up for 2.7 years (HERS II). It was concluded that post-menopausal HRT should not be used to decrease the risk of CHD in women already with CHD. In the past, the protection of women using HRT against cardiovascular disease was considered to be much greater than the negative effect of increased cancer. Just recently, a report[37] from the Women's Health Initiative decided to stop their estrogen plus progestin component post-menopausal women trial. After 5.2 years of follow-up, the report indicated that CHD and invasive breast cancer were primary adverse outcomes of the treatment. It concluded that the overall health risks exceeded the benefits once believed to come from combining estrogen and progestin. It is not yet clear whether alternative forms of HRT can have the desired cardio-protective effects to modify arterial stiffness in a long-term setting. This study will illustrate the results from the two different forms of HRT used, HRT-E and HRT-EP.

2.6 Hormone Replacement Therapy and Arterial Stiffness

The exact mechanisms underlying estrogen-mediated changes in the cardiovascular system are not fully understood. The mechanism by which exogenous estrogen usage after menopause prevents cardiovascular disease is most likely associated to multiple factors[35]. These factors include alterations in lipid profile, endothelium-derived relaxing factor in coronary arteries, and its vasodilatory effects.

Arterial stiffness, quantified in terms of *PWV*, has been seen to increase with age in both men and women[38-40]. Following menopause, this aging-associated increase in *PWV* in women appears to accelerate[13,38]. A study of hypertensive women also found a rapid decrease in compliance at perimenopause and has related this to changes in endogenous estrogen levels[2]. Thus, the loss of estrogen at menopause is one of the likely explanations for the increased arterial stiffness as quantified by increased *PWV* or decreased arterial compliance. Experimental animal and human studies have shown that estrogen administration has a vasodilatory effect and also results in structural changes in large and coronary arteries[41]. Estrogen has been found to cause a rapid release of nitric oxide in cultured endothelial cells[3]. Alterations in endothelium-derived relaxing factor support the idea that estrogen affects vascular tone via the nitric oxide pathway. Endothelial nitric oxide synthase (eNOS) is stimulated by estrodial via nongenomic actions of estrogen receptor α (ERα)[42]. Estrodial is an important agonist for endothelial nitric oxide synthase (eNOS) in both physiologic and pathophysiological conditions, especially in our case, affecting arterial stiffness in post-menopausal women receiving HRT[43]. Local administration of estrogen causes immediate vasodilatory responses in

large arteries, while actual structural changes take a longer time[41]. Preliminary reports have indicated a reduction in arterial stiffness with short-term intravenous administration of estrogenic compounds in a group of post-menopausal women[44].

Long-term treatment with estrogen-containing hormonal therapy has been shown to partially reverse the increase in arterial stiffness and may contribute to a lowering of cardiovascular risk factors (e.g., incidence of myocardial ischemia) [34]. Estrogen does have direct effects on vascular connective tissue degradation[45] and inhibition of vascular smooth muscle cells[46]. These findings suggest that long-term estrogen administration should have a favorable influence on arterial stiffness via vascular remodeling. However, a long-term study of post-menopausal usage of the synthetic steroid Tibolone, which is structurally related to norethisterone, did not alter arterial compliance, as quantified by aortic *PWV*[47].

Estrogen receptors have been discovered in the cardiovascular system of certain animals, baboons and rats, and also in humans, while progesterone receptors have been identified in the human heart and great vessels[35]. Animal data have supported the hypothesis that estrogen targets the cardiovascular system and plays a role in regulating cardiovascular cell function and cardiovascular remodeling[48]. A finding discussing the atherosclerotic coronary arteries of pre-menopausal women also supported this hypothesis. This finding illustrated that there was a decrease in the number of estrogen receptors in smooth muscle cells in women with atherosclerosis when compared to similar women with no atherosclerosis[49]. Post-menopausal estrogen usage in women has been linked to a decline in the common carotid artery wall thickness and decreasing occurrence of subclinical carotid stenosis when compared with those women who had

never used estrogen[50]. Therefore, it seems that post-menopausal estrogen usage in women may be beneficial in lowering the risk of cardiovascular disease.

2.7 Background Summary

The arterial system hydraulic load (i.e., the opposition to movement of blood out of the ventricle) consists of steady (i.e., *SVR*) and pulsatile components. Vascular stiffness (elastic property) is a major determinant of the pulsatile load. Menopause accelerates the age-associated increase in arterial stiffness[13,38]. There is evidence that pulsatile arterial load plays a role in cardiovascular remodeling and may be an independent cardiovascular risk factor. Finally, estrogen administration results in acute vasodilation and vascular remodeling in the chronic setting. Therefore, an examination of the chronic effects of HRT on pulsatile arterial load, especially vascular stiffness aspects is a worthwhile effort. This is precisely the goal of the present study.

3.0 METHODS

3.1 Study Design

The present study examined the effects of chronic HRT on systemic vascular properties of post-menopausal women. Thirty-five post-menopausal women were studied and divided into two groups: women receiving no hormone replacement therapy (control, n=25) and women receiving hormone replacement therapy (HRT-all, n=10). The HRT-all group was further subdivided into two-subgroups: women receiving estrogen alone (n=5, Premarin, 0.625mg/day of conjugated estrogen, HRT-E) and those women receiving estrogen and progesterone (n=5, Prempro, 0.625mg/day of conjugated estrogen + 2.5 mg/day of medroxyprogesterone acetate, HRT-EP). All subjects in the HRT-E group had previously undergone hysterectomy. The basic demographic characteristics of study participants are shown in Table 1.

Table 1: Subject Characteristics

	Control (n = 25)	HRT-all (n = 10)	
		HRT-E (n = 5)	HRT-EP (n = 5)
Age at study initiation	53±1	49±1	50±1
Age at menopause	49±1	49±1	47±3
Weight (kg)	68±3	70±3	70±5
Height (cm)	166±2	165±1	158±3
Maternal Race			
White Black Asian	18 6 1	3 2 0	4 1 0

Data are mean±SEM

Noninvasive data (tonometric pressures and Doppler-based aortic blood flow waveforms) were collected serially at five different times: once at baseline during the first visit and during four subsequent visits after the initiation of the study at 19±1, 108±5, 193±4, and 388±8 days, respectively. None of the study participants were receiving HRT or any other cardiovascular medications prior to the initiation of the present study.

3.2 Experimental Measurements

All subjects were weighed and underwent noninvasive evaluations to quantify global (*SVR*, *AC*, and wave reflection indices) and regional (*PWV*) properties of systemic arterial circulation. Noninvasive measurements included: (1) electrocardiogram (ECG), (2) brachial artery systolic, diastolic, and mean pressures by automated oscillometric sphygmomanometry, (3) tonometric pressure waveforms at several vascular sites (carotid, femoral, brachial, and radial) using pressure sensors designed for non-invasive recording of pulse pressure wave contours, (4) ascending aortic blood velocity (flow) waveforms using Doppler ultrasound. All studies were performed in the left lateral decubitus position, and data were acquired after the patient had been resting for ten minutes.

3.2.1 Noninvasive Measurement of Pressure Waveform

It is possible to record high-fidelity arterial pressure waveform noninvasively at various locations using applanation tonometry[51-57]. A miniature strain gauge transducer, mounted in a hand-held, pencil-probe (SPT-301, Millar Instruments), was used to record pressures from right carotid, right brachial, and left femoral sites. All analog pressure data was digitized on-line at 1000 Hz using a portable PC-based data acquisition system. An automated, wrist-worn tonometer was used to record pressure waveform data from the right radial site (Pilot 9200, Colin Medical Instruments Corp.). Pressure waveforms were calibrated using brachial artery blood pressures determined with an oscillometric sphygmomanometer, with the pressure cuff located on the left arm (Pilot 9200, Colin Medical Instruments Corp.). The brachial artery pressure waveform was calibrated first by assigning the systolic and diastolic brachial pressures to the maximum and minimum of the waveform, respectively. The mean arterial pressure (*MAP*) was computed from the calibrated brachial artery pressure waveform and assumed to be the same for all other locations (i.e., carotid, femoral, and radial). One more calibration point is needed in order to fully calibrate pressure waveforms at these other locations. It was assumed that that diastolic pressures were the same at different locations, an assumption that is supported by experimental data[56,58]. Simultaneously recorded pairs of pressure waveforms (carotid and femoral; brachial and radial) are illustrated in Figure 5.

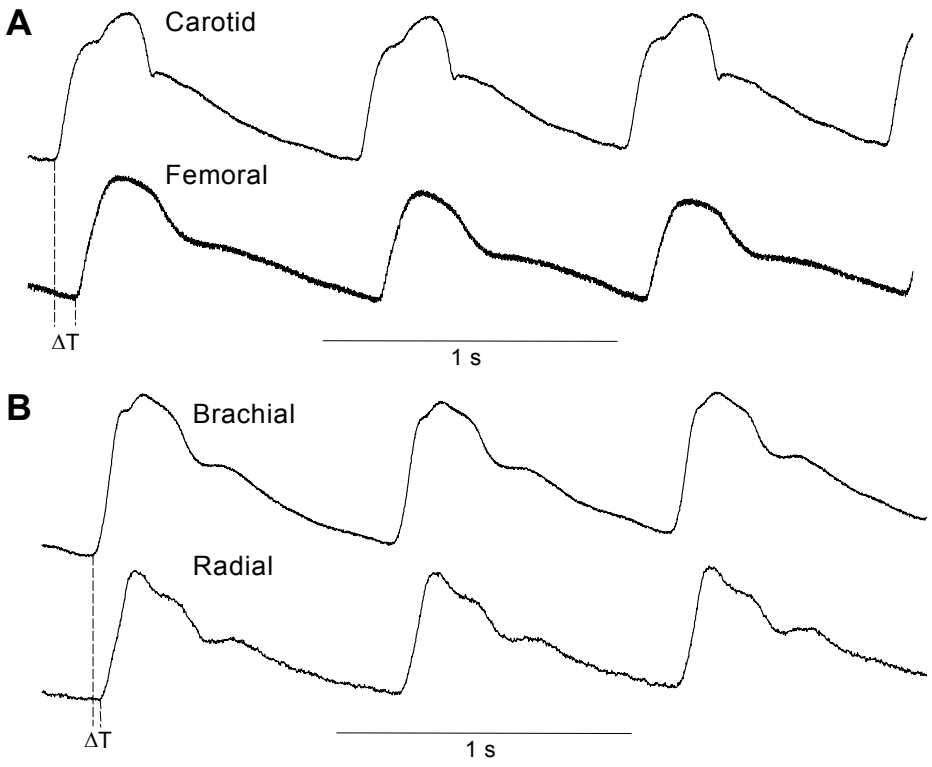

Figure 5: Noninvasive and simultaneous measurements of pressure waveforms at two sites using tonometers. A: carotid and femoral; B: brachial and radial. ΔT = time-delay between the two pressure waveforms.

3.2.2 Noninvasive Measurement of Ascending Aortic Flow Waveform

Noninvasive instantaneous ascending aortic flow data were obtained from the measurements of aortic blood velocity and left ventricular outflow tract diameter (D_{LVOT}) (Figure 6). Aortic blood velocity was recorded from the cardiac apex using a two-dimensionally guided pulsed wave Doppler (Hewlett Packard, SONOS-5000, 2.5 Mhz phased-array & 7.5 or 12 Mhz linear). The instantaneous velocity signals were recorded on paper and then digitized using custom-built software. The instantaneous volumetric blood flow was calculated as the product of measured instantaneous blood velocity and

cross-sectional area (= $\pi D^2_{LVOT}/4$). This calculation assumes a flat velocity profile and negligible variation in D_{LVOT} over the cardiac cycle at the ascending aorta. A typical example of simultaneous ECG, carotid pressure waveform, and echocardiographic view of LV outflow tract diameter is illustrated in Figure 6.

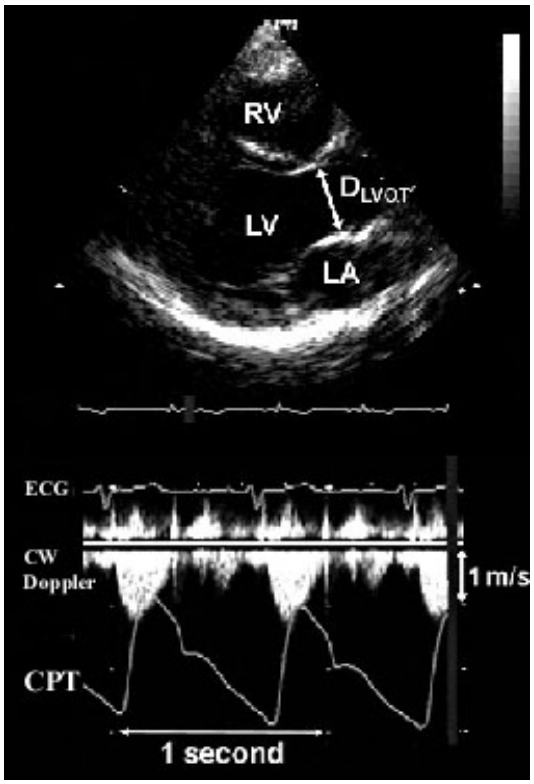

Figure 6: 2D echocardiographic view of LV outflow tract diameter (top). Simultaneous electrocardiogram (ECG), carotid pressure (CPT), and aortic flow velocity (CW Doppler) tracings

3.3 Calculations of Derived Variables

3.3.1 Global Systemic Arterial Mechanical Properties

Aortic input impedance spectrum (Z_{in}). As discussed before Z_{in} is a comprehensive characterization of the mechanical properties of the entire systemic arterial circulation. Z_{in} was calculated from the measured aortic pressure [$P_{ao}(t)$] and flow [$Q_{ao}(t)$] waveforms using standard harmonic analysis techniques[12]. Since the carotid pressure waveform was used as a proxy for ascending aortic pressure waveform, the calculations should be considered an estimate of the true aortic input impedance. *SVR* was calculated as being Z_{in} at zero Hz (which is identical to *MAP* divided by *CO*), Z_c was calculated from the average of the Z_{in} magnitudes over 4-12 Hz. Those frequencies with flow magnitudes smaller than 5% of the first harmonic was excluded from this averaging process. This eliminates impedance values that are due to insufficient energy in the flow harmonic, which can cause estimation errors.

Global arterial compliance (AC). *AC,* a quantity that is inversely proportional to arterial stiffness, was estimated from the diastolic decay of the aortic pressure waveform by the area method[11,14].

$$AC = \frac{A_d}{SVR(P_1 - P_2)}, \tag{3-1}$$

where P_1 and P_2 are pressures at the beginning (i.e., peak pressure following the dicrotic notch) and the end (end diastolic pressure) of the diastolic decay region and A_d is the area underneath the diastolic portion of the pressure waveform (Figure 7). This estimation

procedure assumes pressure-independent compliance, a reasonable assumption when comparing compliance data between groups with small pressure differences. However when pressure differences are large, a pressure-dependent compliance model must be used for calculating *AC*. This was not necessary in the present study. Our expectation was that *AC* would increase in patients receiving HRT.

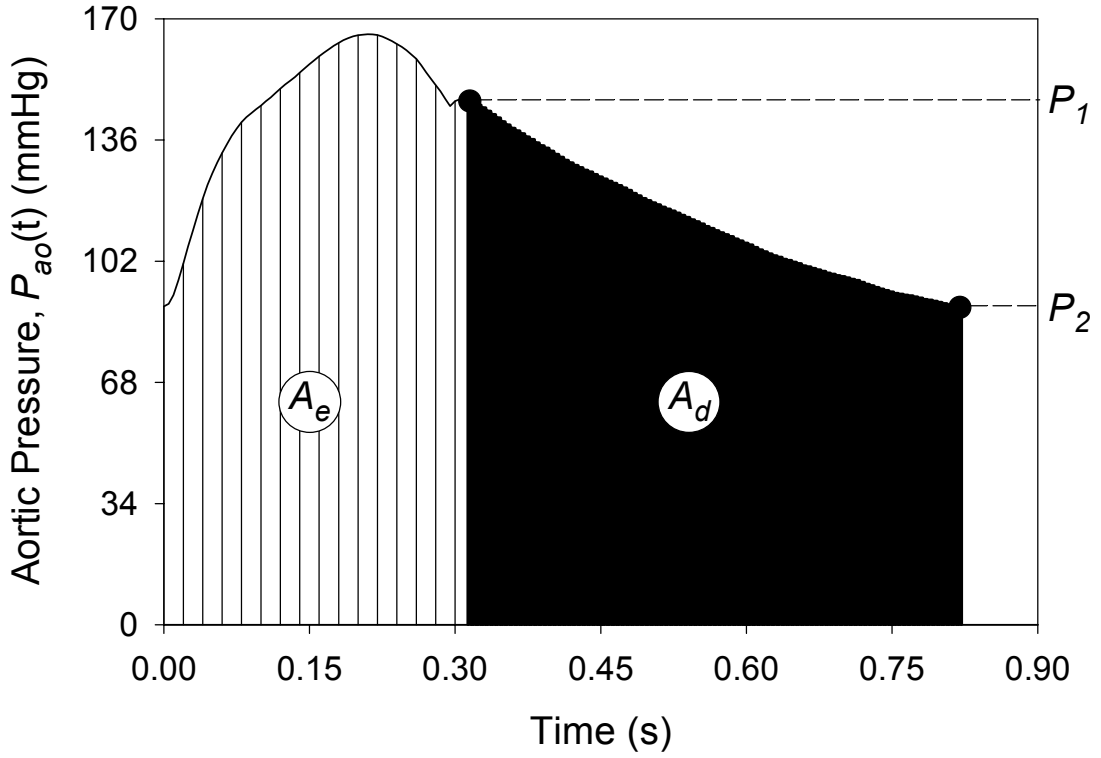

Figure 7: Calculation of global arterial compliance using the area method

Global arterial wave reflections. Two indices were calculated for this purpose: reflection index (*RI*), calculated as the ratio of the backward and forward pressure wave peak-to-peak amplitudes[18], and the magnitude of the first harmonic of global reflection coefficient ($|\Gamma_1|$), derived from the estimated input impedance spectrum and aortic characteristic impedance[12].

Hydraulic power. Instantaneous pressure and flow data were used to calculate total (W_{tot}), steady ($W_{std} = MAP*CO$), and oscillatory ($W_{osc} = W_{tot} - W_{std}$) power[12]:

$$W_{tot} = \frac{1}{T}\int_0^T P(t)Q(t)dt\,, \tag{3-2}$$

where T is the cardiac cycle duration. W_{osc} is power that is wasted during pulsations; the ratio of W_{osc} and W_{tot} was used as a measurement of the inefficiency of the LV-arterial coupling. A Fortran program was developed previously by Dr. Shroff in order to calculate all of the quantities from the digitized pressure-flow waveforms.

3.3.2 Regional Arterial Mechanical Properties

Pulse wave velocity (PWV). *PWV* was calculated from the simultaneous measurements of pressure waveforms at two sites (e.g., carotid and femoral; brachial and radial) and distance between the sites (Figure 5). The time delays between carotid and femoral ($\Delta T_{C\text{-}F}$) and brachial and radial ($\Delta T_{B\text{-}R}$) pressure waveforms were computed using a computerized algorithm (intersecting tangent method) that was previously created[59]. Three physical distances were measured by following the typical vascular pathways on the body surface: heart (i.e., aortic valve plane identified by echocardiography) to right carotid ($D_{H\text{-}C}$), heart to left femoral ($D_{H\text{-}F}$), and right brachial to right radial ($D_{B\text{-}R}$). Carotid-to-femoral ($PWV_{C\text{-}F}$) and brachial-to radial ($PWV_{B\text{-}R}$) *PWVs* were calculated as follows.

$$PWV_{C-F} = \frac{D_{H-F} - D_{H-C}}{\Delta T_{C-F}}, \qquad PWV_{B-R} = \frac{D_{B-R}}{\Delta T_{B-R}}. \tag{3-3}$$

Our expectation was that *PWV* would decrease (indicating reduced arterial stiffness or increased compliance) in patients receiving HRT. Quantification of $PWV_{C\text{-}F}$ and $PWV_{B\text{-}R}$ would allow for monitoring regional vascular stiffness changes, the former representing stiffness of large central vessels and the latter representing stiffness of smaller peripheral vessels.

3.4 Statistical Analysis

All statistical analyses were performed using a PC-based software (GB-Stat for Windows). Data were normalized to the first visit representing baseline values. For each parameter, a two-way ANOVA (factor 1: therapy status, control and HRT-all or control, HRT-E, and HRT-EP; factor 2: time, five visits) with repeated measures on factor-2 was used to analyze data. When necessary, post-hoc analysis was performed to further characterize the observed differences. Specifically, temporal changes within each therapy group were analyzed by comparing the normalized values during Visits 2-5 versus 1 (which is the normalized value at baseline or Visit 1) using the Dunnett's test. In addition, differences between the control group and the HRT groups at matched time points (i.e., at Visits 2, 3, 4, and 5) were examined using pairwise comparisons (8 comparisons in our case), with the P value adjusted for multiple comparisons (Bonferroni correction). A *P* value of less than 0.05 for the set of all comparisons was taken to indicate statistically significant differences. Data are presented as mean±SEM.

4.0 RESULTS

4.1 Hemodynamic Variables

Group-averaged hemodynamic data are presented in Table 2-6. Graphical representations of relative changes in these hemodynamic variables are illustrated in Figure 8-14. It should be noted that although a straight line connects successive measured data points, this should not be taken to represent actual temporal changes between measurement points. Heart rate (*HR*), stroke volume (*SV*), and cardiac output (*CO*) did not change significantly in the control group throughout the study period (Figure 8-10). This was also true for both HRT groups, except for a small decrease in *HR* at Visits 3 and 4 for the HRT-E group (Figure 8) and an increase in *CO* at Visit 3 in the HRT-EP group (Figure 10). Mean arterial pressure (*MAP*) decreased over time in both the control and the two HRT groups, reaching statistical significance at the fifth visit (Figure 11). Carotid peak systolic ($P_{s\text{-}carotid}$) and minimum diastolic pressures (P_d) tended to decrease over time as well, but these changes did not reach statistical significance (Figure 12 and 14).

Table 2: General Hemodynamics, Visit 1

	Control	HRT-all	HRT-E	HRT-EP
HR, bpm	75±3	78±3	84±2	73±4
CO, L/min	4.9±0.2	5.0±0.2	4.9±.3	5.0±0.4
SV, mL	66±3	64±2	59±3	68±3
MAP, mmHg	87±1	88±2	87±3	88±2
$P_{s\text{-}carotid}$, mmHg	110±2	109±3	109±5	109±3
P_d, mmHg	70±1	70±1	69±1	70±2
$P_{s\text{-}brachial}$, mmHg	123±2	121±3	120±5	122±2

Table 3: General Hemodynamics, Visit 2

	Control	HRT-all	HRT-E	HRT-EP
HR, bpm	73±2	72±3	76±3	68±4
CO, L/min	4.9±0.2	4.7±0.1	4.6±0.1	4.9±0.2
SV, mL	69±3	67±4	60±2	73±6
MAP, mmHg	84±2	83±2	85±3	81±2
$P_{s\text{-}carotid}$, mmHg	104±2	106±3	108±5	103±2
P_d, mmHg	68±2	65±2	66±3	64±3
$P_{s\text{-}brachial}$, mmHg	118±2	116±3	118±5	114±3

Table 4: General Hemodynamics, Visit 3

	Control	HRT-all	HRT-E	HRT-EP
HR, bpm	71±2	76±2	73±3	79±4
CO, L/min	4.8±0.2	5.2±0.3	4.6±0.1	6.0±0.5
SV, mL	67±3	68±3	62±1	75±5
MAP, mmHg	85±2	85±2	85±2	84±3
$P_{s\text{-}carotid}$, mmHg	106±2	106±3	109±5	103±4
P_d, mmHg	68±2	67±2	67±1	67±3
$P_{s\text{-}brachial}$, mmHg	120±2	119±3	117±4	121±4

Table 5: General Hemodynamics, Visit 4

	Control	HRT-all	HRT-E	HRT-EP
HR, bpm	72±3	73±3	73±2	74±5
CO, L/min	4.8±0.2	5.0±0.3	4.6±0.5	5.3±0.3
SV, mL	68±3	68±4	64±7	72±3
MAP, mmHg	83±2	83±1	82±1	83±2
$P_{s\text{-}carotid}$, mmHg	105±3	103±3	105±5	102±3
P_d, mmHg	65±2	65±1	65±2	66±2
$P_{s\text{-}brachial}$, mmHg	116±2	118±2	116±5	119±2

Table 6: General Hemodynamics, Visit 5

	Control	HRT-all	HRT-E	HRT-EP
HR, bpm	72±3	74±2	78±3	70±2
CO, L/min	4.9±0.2	4.8±0.2	4.9±0.4	4.7±0.1
SV, mL	68±3	65±2	62±3	68±3
MAP, mmHg	83±2	82±1	84±3	81±2
$P_{s\text{-}carotid}$, mmHg	103±3	103±1	103±1	103±3
P_d, mmHg	66±0	65±2	68±4	62±2
$P_{s\text{-}brachial}$, mmHg	118±2	113±3	121±1	113±3

HR indicates heart rate; *CO*, cardiac output; *SV*, stroke volume; $P_{s\text{-}carotid}$, carotid peak systolic pressure; P_d, carotid or brachial minimum diastolic pressure; $P_{s\text{-}brachial}$, brachial peak systolic pressure. Data are mean±SEM.

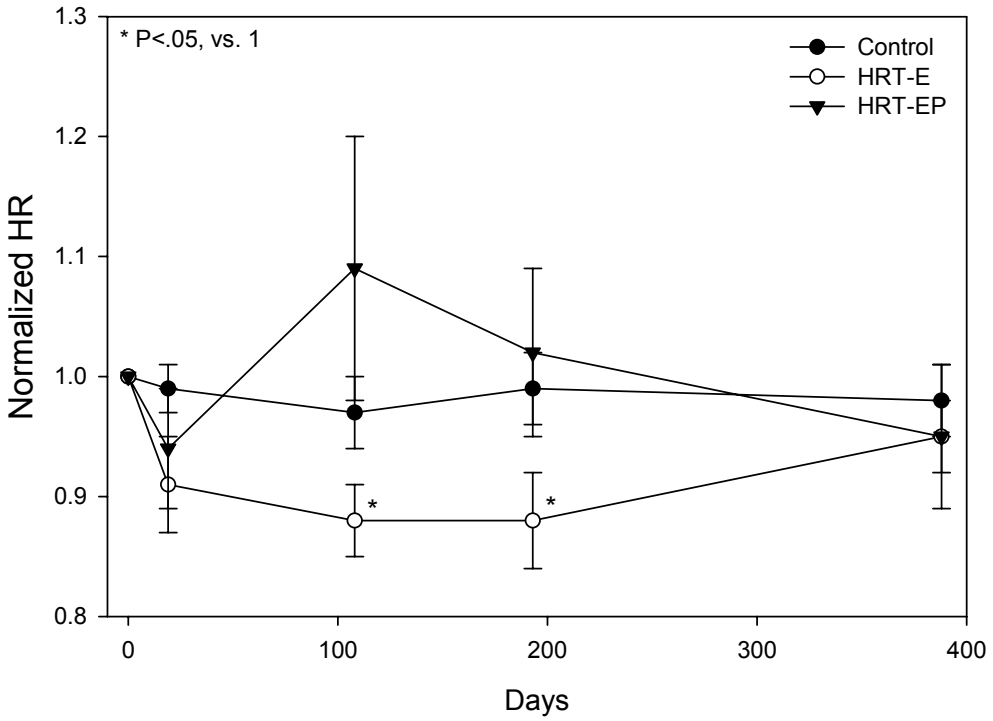

Figure 8: Normalized heart rate responses
All figures are normalized to the first visit (baseline) of each respective group.

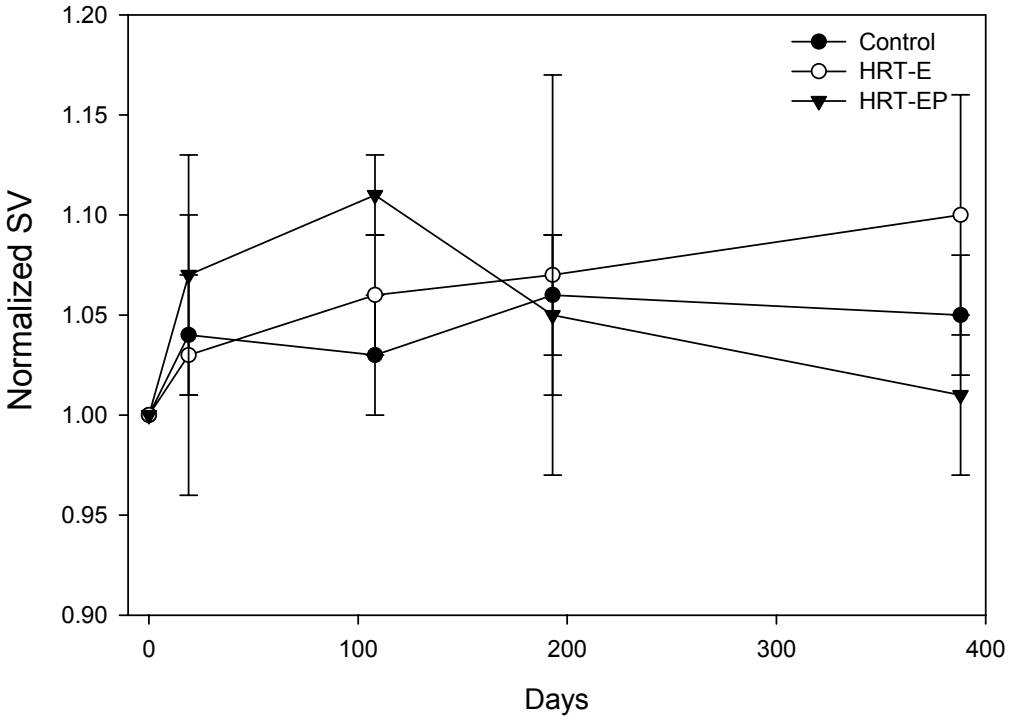

Figure 9: Normalized stroke volume responses

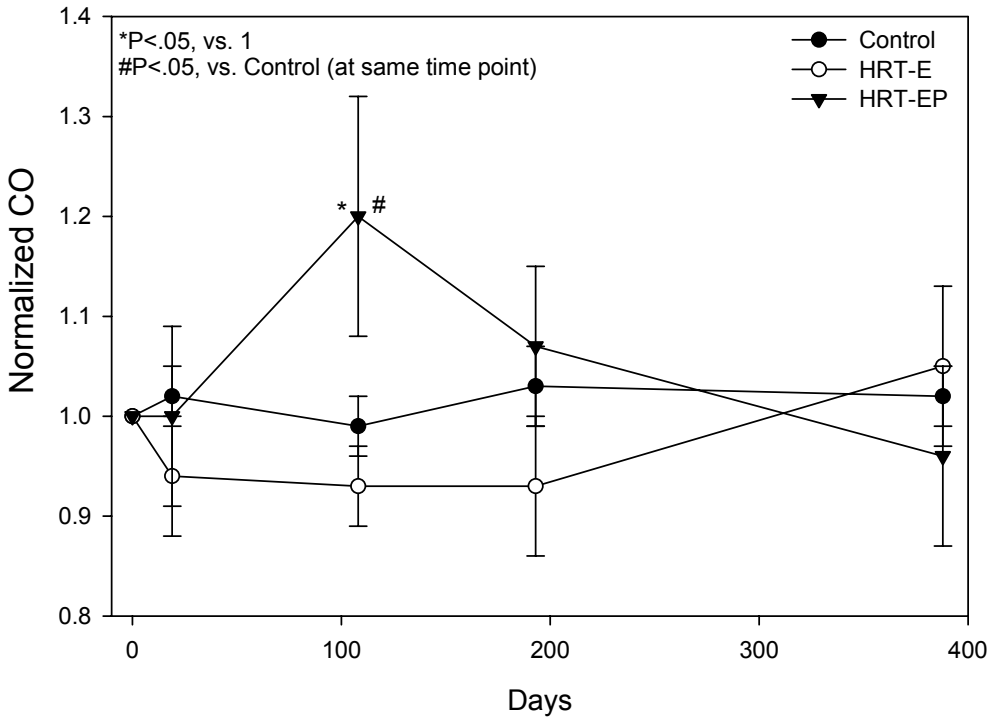

Figure 10: Normalized cardiac output responses

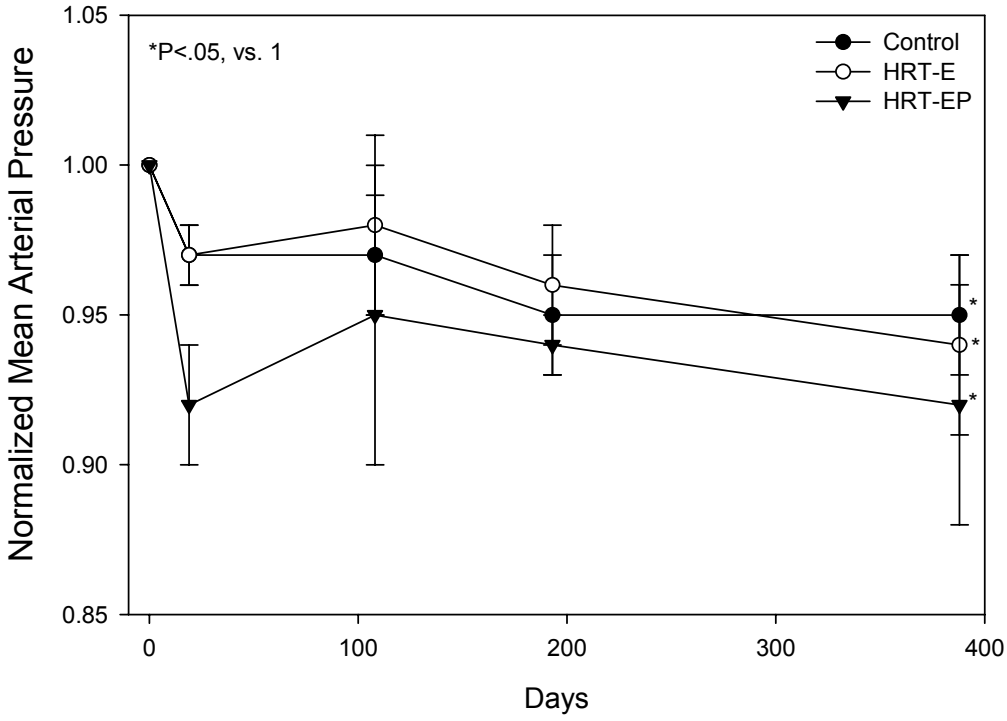

Figure 11: Normalized mean arterial pressure responses

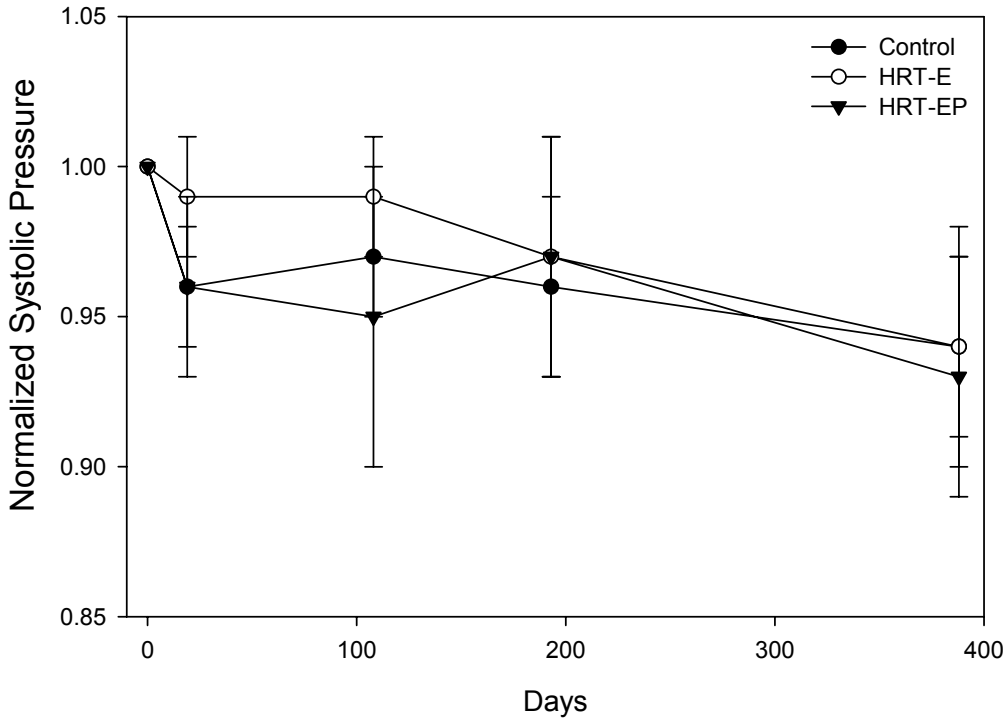

Figure 12: Normalized carotid (aortic) peak systolic blood pressure responses

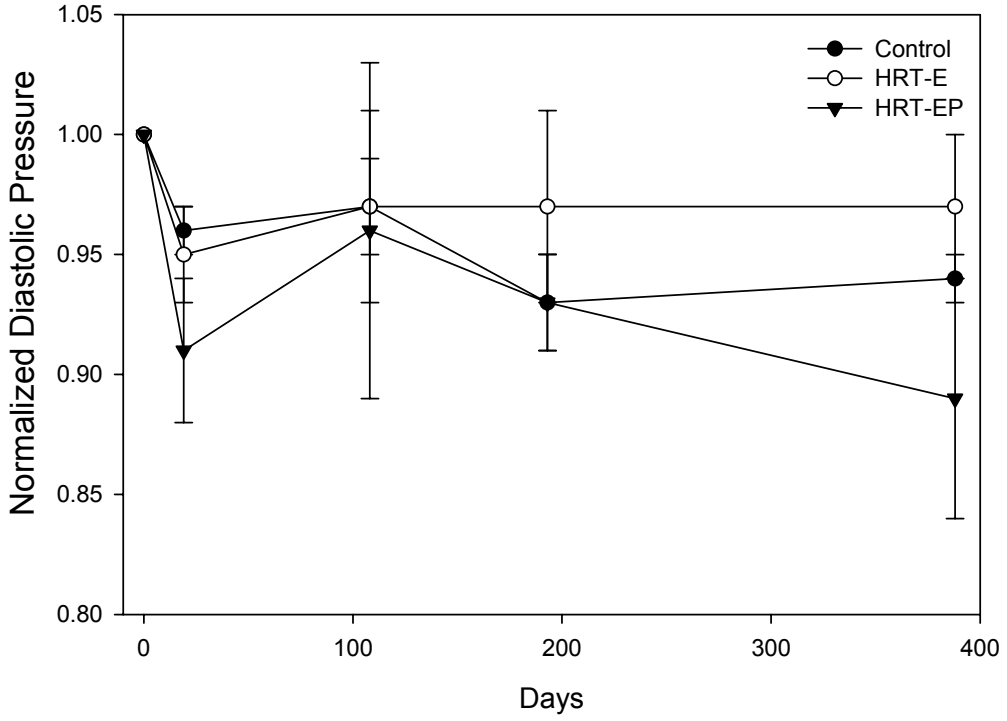

Figure 13: Normalized minimum diastolic blood pressure responses

4.2 Global Systemic Arterial Mechanical Properties

We first examined the input impedance spectrum (Z_{in}) because it provides a comprehensive characterization of global systemic arterial mechanical properties. The magnitude of Z_{in} as a function of frequency for the control and two HRT groups are illustrated in Figure 14-17. For the sake of clarity, data from only three visits are shown in each of these figures. There are no clear changes in the magnitude of Z_{in} over time for the control and HRT-EP groups. The magnitude of Z_{in} appears to fall over time for the HRT-E group, especially at low frequencies (i.e., below 3 Hz). We will now examine the various aspects of Z_{in} (e.g., *SVR*, *AC*, Z_c, Z_1, reflection indices) in more detail.

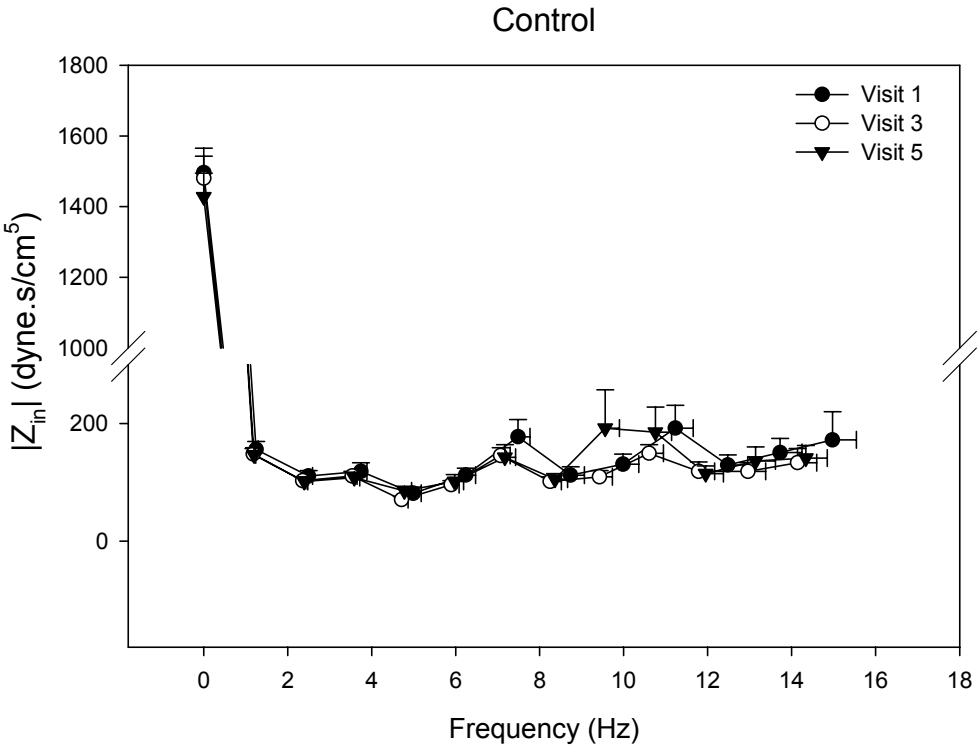

Figure 14: Magnitude of Z_{in} for the control group at three selected visits

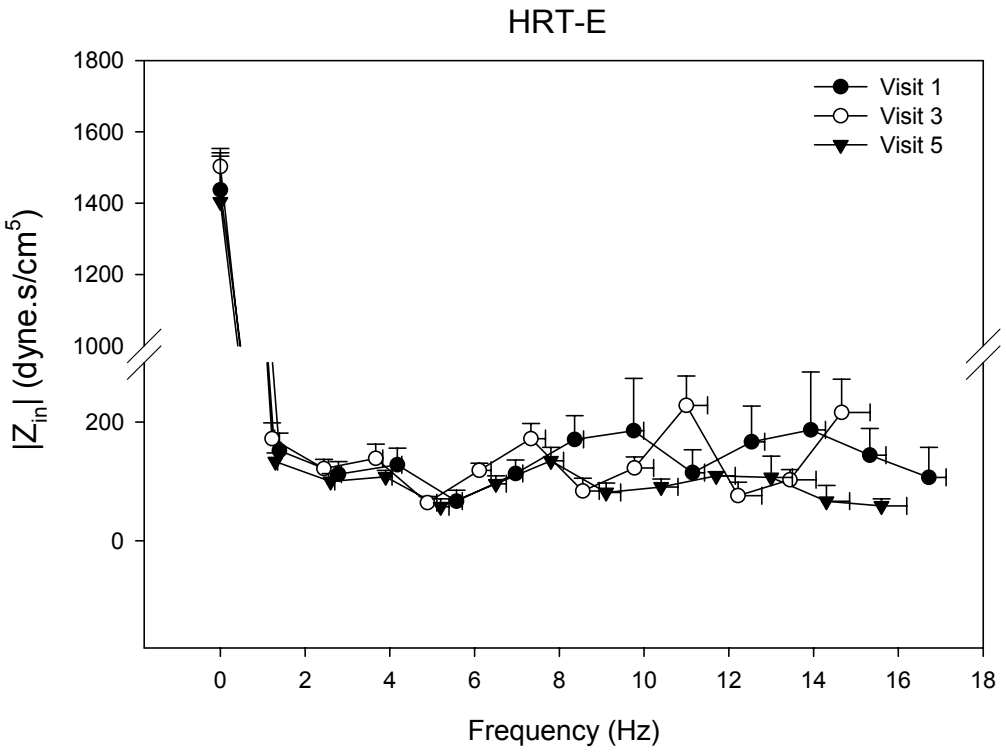

Figure 15: Magnitude of Z_{in} for the HRT-E group at three selected visits

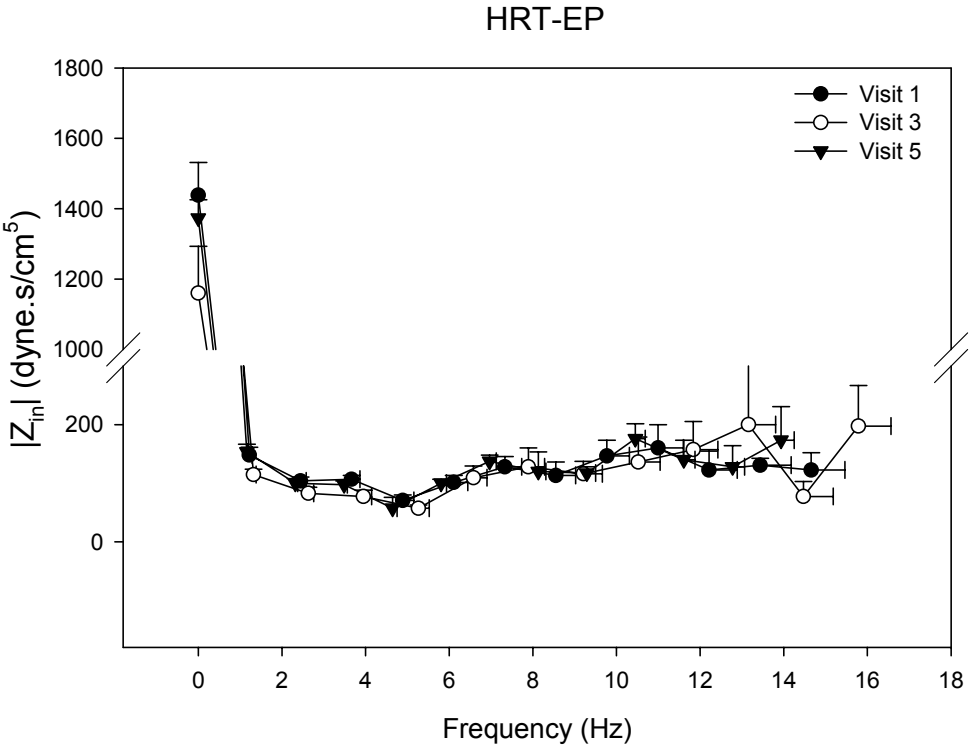

Figure 16: Magnitude of Z_{in} for the HRT-EP group at three selected visits

Group-averaged data for global systemic arterial characterization are presented in Table 7-11. Graphical representations of relative changes in selected systemic arterial mechanical properties are illustrated in Figure 17 and 18.

Total systemic vascular resistance (SVR). Overall, *SVR* did not change significantly in either the control or the HRT groups (Figure 17), except for one isolated decrease in *SVR* at Visit 3 for the HRT-EP group (Figure 17).

Global arterial compliance (AC). *AC* was unchanged for the control and HRT-EP groups. In contrast, *AC* increased in the HRT-E group, reaching statistical significance at the fifth visit (Figure 18).

First harmonic of input impedance spectrum (Z_1) and reflection indices. Z_1 and both indices of global arterial reflections did not change significantly in either the control or the HRT groups.

Hydraulic power. W_{tot}, W_{std}, *and* W_{osc} indices of hydraulic power of the efficiency of the left ventricle did not change significantly in either the control or the HRT groups.

Table 7: Global Systemic Arterial Characterization, Visit 1

	NO HRT	HRT	HRT-E	HRT-EP
SVR, dyne.s/cm^5	1493±67	1440±67	1440±107	1440±93
AC, mL/mmHg	1.81±0.13	1.58±0.12	1.54±0.25	1.61±0.06
Z_1, dyne.s/cm^5	155±14	150±15	152±30	148±13
RI	0.47±0.02	0.47±0.02	0.45±0.03	0.48±0.02
$\lvert\Gamma_1\rvert$	0.43±0.02	0.44±0.02	0.45±0.04	0.44±0.03
W_{tot}, mW	1069±69	1123±48	1115±59	1130±84
W_{std}, mW	912±59	967±44	957±51	978±78
W_{osc}, mW	156±15	155±12	158±25	152±8
$\%W_{osc}$	15%	14%	14%	13%

Table 8: Global Systemic Arterial Characterization, Visit 2

	NO HRT	HRT	HRT-E	HRT-EP
SVR, dyne.s/cm^5	1426±67	1413±53	1493±80	1333±53
AC, mL/mmHg	1.86±0.13	1.65±0.13	1.47±0.17	1.83±0.16
Z_1, dyne.s/cm^5	139±9	160±15	170±23	151±21
RI	0.47±0.02	0.50±0.01	0.50±0.01	0.50±0.02
$\lvert\Gamma_1\rvert$	0.45±0.02	0.44±0.02	0.46±0.01	0.42±0.03
W_{tot}, mW	1071±43	1036±39	1022±53	1050±63
W_{std}, mW	923±37	872±30	863±30	880±56
W_{osc}, mW	148±10	164±19	159±28	170±28
$\%W_{osc}$	14%	16%	16%	16%

Table 9: Global Systemic Arterial Characterization, Visit 3

	NO HRT	HRT	HRT-E	HRT-EP
SVR, dyne.s/cm^5	1480±67	1346±80	1506±53	1160±133
AC, mL/mmHg	1.77±0.10	1.35±0.10	1.47±0.14	1.92±0.11
Z_1, dyne.s/cm^5	148±10	147±18	172±27	115±9
RI	0.48±0.02	0.46±0.02	0.47±0.02	0.45±0.04
$\lvert\Gamma_1\rvert$	0.46±0.02	0.43±0.02	0.45±0.02	0.40±0.03
W_{tot}, mW	1048±46	1133±67	1021±40	1273±113
W_{std}, mW	900±40	971±60	864±30	1106±98
W_{osc}, mW	149±10	162±12	157±20	167±15
$\%W_{osc}$	14%	14%	15%	13%

Table 10: Global Systemic Arterial Characterization, Visit 4

	NO HRT	HRT	HRT-E	HRT-EP
SVR, dyne.s/cm^5	1413±53	1360±93	1493±173	1266±53
AC, mL/mmHg	1.72±0.15	1.92±0.25	1.88±0.47	1.95±0.29
Z_1, dyne.s/cm^5	153±9	145±17	168±35	127±14
RI	0.49±0.02	0.44±0.02	0.46±0.03	0.43±0.02
$\lvert\Gamma_1\rvert$	0.45±0.02	0.40±0.02	0.41±0.03	0.40±0.03
W_{tot}, mW	1059±57	1072±63	994±97	1135±81
W_{std}, mW	899±45	913±57	839±88	972±72
W_{osc}, mW	160±15	160±16	155±26	163±22
$\%W_{osc}$	15%	15%	16%	14%

Table 11: Global Systemic Arterial Characterization, Visit 5

	NO HRT	HRT	HRT-E	HRT-EP
SVR, dyne.s/cm^5	1426±67	1386±67	1400±133	1373±53
AC, mL/mmHg	1.90±0.16	1.67±0.09	1.82±0.13	1.52±0.07
Z_1, dyne.s/cm^5	147±12	143±10	134±14	153±13
RI	0.48±0.02	0.49±0.02	0.48±0.03	0.50±0.02
$\lvert\Gamma_1\rvert$	0.45±0.02	0.46±0.02	0.45+0.03	0.47+0.04
W_{tot}, mW	1045±60	1022±40	1044±77	1001±35
W_{std}, mW	893±50	876±32	902±61	851±23
W_{osc}, mW	152±14	146±15	142±28	150±17
$\%W_{osc}$	15%	17%	14%	15%

SVR indicates total systemic vascular resistance; *AC*, global arterial compliance; Z_1, modulus of first (fundamental) harmonic of the input impedance spectrum; *RI*, reflection index; $\lvert\Gamma_1\rvert$, magnitude of the first harmonic of the global reflection coefficient spectrum; W_{tot}, total power; W_{std}, steady power; W_{osc}, oscillatory power; $\%W_{osc}$, percent oscillatory power. Data are mean±SEM.

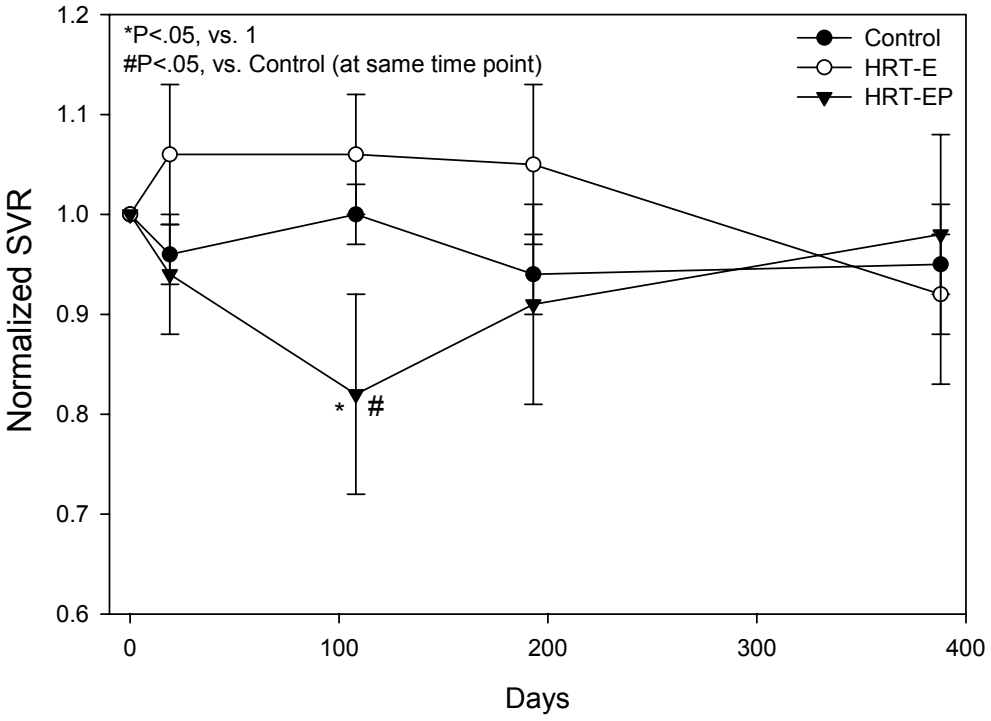

Figure 17: Normalized total systemic vascular resistance responses

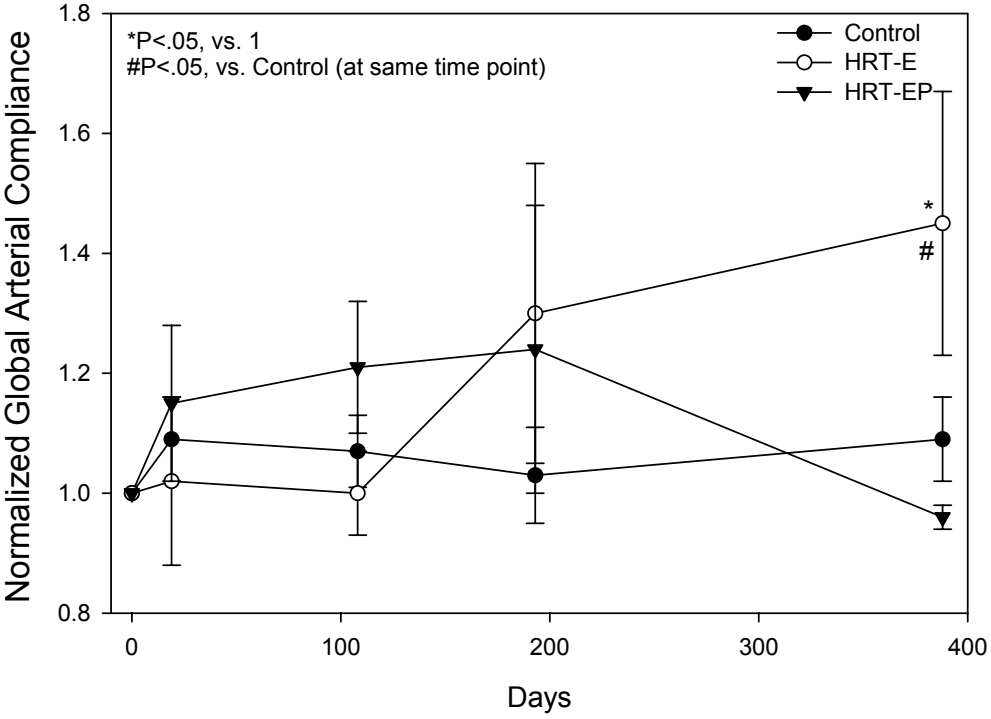

Figure 18: Normalized global arterial compliance responses

4.3 Regional Arterial Mechanical Properties

Group averaged *PWV* data are presented in Table 12-16 and graphical representations of relative changes in *PWV* data are illustrated in Figure 19 and 20.

Carotid-to-femoral pulse wave velocity (PWV_{C-F}). For the control group, PWV_{C-F} seemed to increase over time, with a statistical significance observed at the fourth visit (~ 6 months). This is consistent with the age-associated increase in vascular stiffness. This age-associated increase in PWV_{C-F} was significantly blunted in the HRT-E group during the early phases of the therapy (Figure 19). However, estrogen-mediated decrease in PWV_{C-F} seemed to wane at the late stage of therapy (> 1 year). The addition of progesterone (HRT-EP group) mitigated the estrogen-mediated decrease in PWV_{C-F} during the early phases; however, the late responses for the two groups (HRT-E and HRT-EP) were similar (Figure 19).

Brachial-to-radial pulse wave velocity (PWV_{B-R}). No significant temporal changes in PWV_{B-R} were observed in the control group. In contrast, PWV_{B-R} began to decrease after the initiation of HRT-E, reaching statistical significance at the fourth visit (~ 6 months). However, this trend appeared to reverse during the late stages of the therapy (Figure 20). The addition of progesterone (HRT-EP group) significantly mitigated the estrogen-mediated decrease in PWV_{B-R} (Figure 20).

Aortic characteristic impedance (Z_c). There were no significant changes in Z_c over time for the control and both HRT groups (Table 12-16).

Table 12: Regional Arterial Mechanical Characterization, Visit 1

	Control	HRT-all	HRT-E	HRT-EP
$PWV_{C\text{-}F}$, cm/s	680±32	704±40	710±31	732±53
$PWV_{B\text{-}R}$, cm/s	798±50	801±39	849±69	754±32
Z_c, dyne.s/cm^5	113±13	105±12	104±24	106±3

Table 13: Regional Arterial Mechanical Characterization, Visit 2

	Control	HRT-all	HRT-E	HRT-EP
$PWV_{C\text{-}F}$, cm/s	719±40	663±48	613±47	726±88
$PWV_{B\text{-}R}$, cm/s	684±45	718±64	669±61	779±127
Z_c, dyne.s/cm^5	96±6	111±10	110±13	112±16

Table 14: Regional Arterial Mechanical Characterization, Visit 3

	Control	HRT-all	HRT-E	HRT-EP
$PWV_{C\text{-}F}$, cm/s	707±50	708±32	633±29	778±35
$PWV_{B\text{-}R}$, cm/s	725±29	768±53	696±85	857±11
Z_c, dyne.s/cm^5	100±6	107±8	113±10	99±14

Table 15: Regional Arterial Mechanical Characterization, Visit 4

	Control	HRT-all	HRT-E	HRT-EP
$PWV_{C\text{-}F}$, cm/s	781±43	667±26	650±36	680±40
$PWV_{B\text{-}R}$, cm/s	816±48	755±73	605±92	875±79
Z_c, dyne.s/cm^5	107±8	118±15	111±18	124±23

Table 16: Regional Arterial Mechanical Characterization, Visit 5

	Control	HRT-all	HRT-E	HRT-EP
$PWV_{C\text{-}F}$, cm/s	736±69	752±57	721±98	780±59
$PWV_{B\text{-}R}$, cm/s	848±106	808±83	755±131	878±102
Z_c, dyne.s/cm^5	108±10	98±8	86±11	110±12

$PWV_{C\text{-}F}$ indicates carotid-to-femoral pulse wave velocity; $PWV_{B\text{-}R}$ brachial-to-radial pulse wave velocity; Z_c, aortic characteristic impedance. Data are mean±SEM.

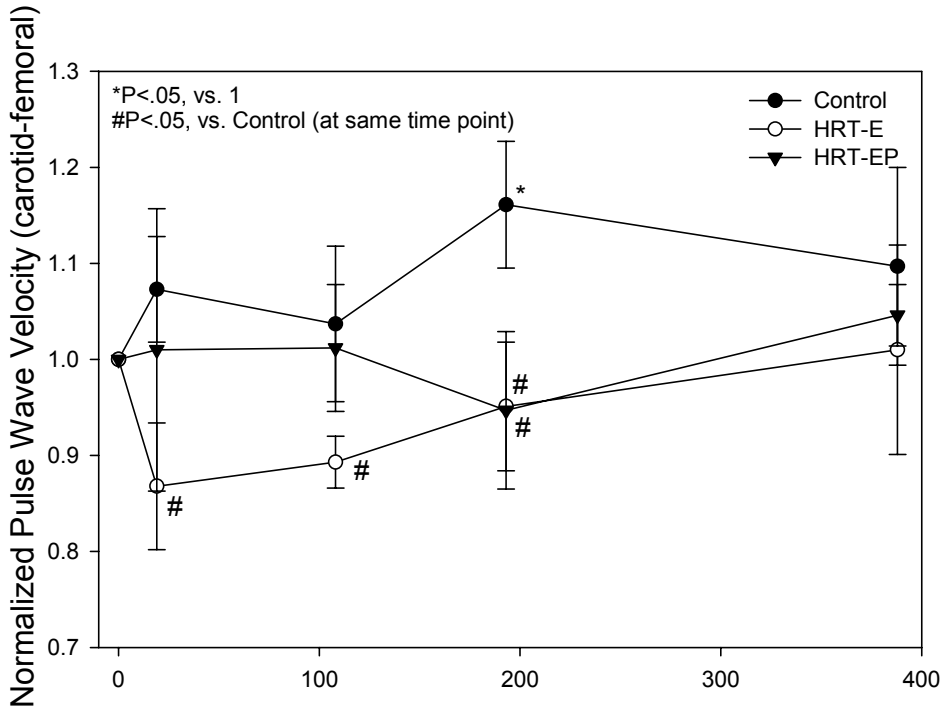

Figure 19: Normalized carotid-to-femoral *PWV* responses

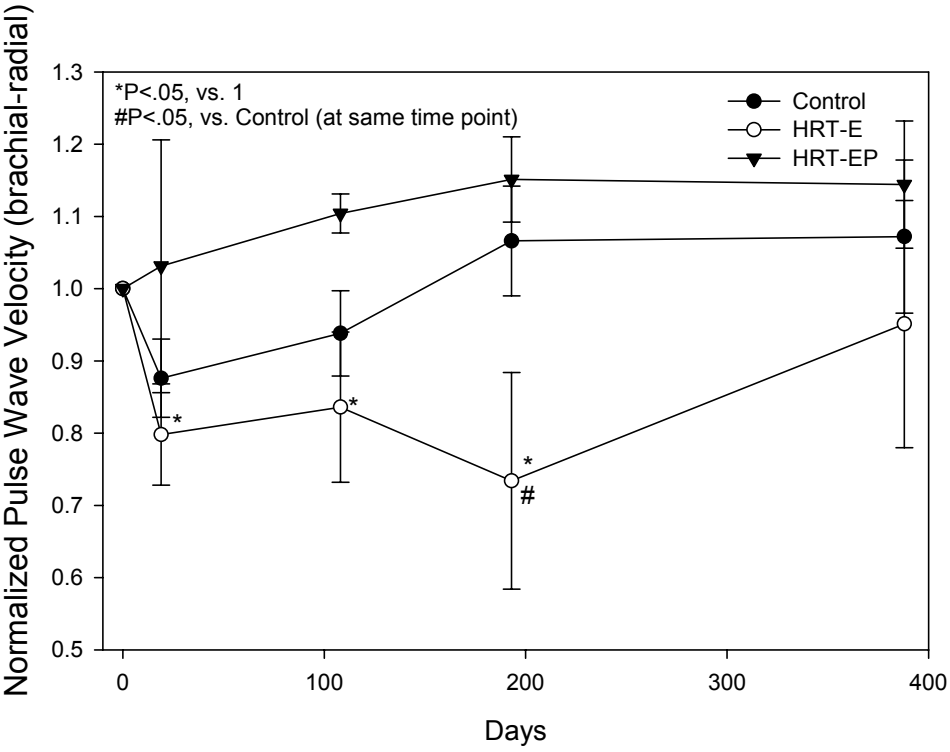

Figure 20: Normalized brachial-to-radial *PWV* responses

5.0 DISCUSSION

5.1 Main Observations

The goal of this present study was to examine the long-term effects of hormone replacement therapy on systemic arterial hemodynamics and mechanical properties, especially arterial stiffness, in post-menopausal women. This was accomplished by studying thirty-five post-menopausal women over a period of approximately one year.

The main result of the present study is that chronic HRT reduces vascular stiffness, as indicated by an increase in *AC* and a decrease in *PWV*, only in the group receiving estrogen alone (HRT-E). When investigating hemodynamic responses to chronic HRT, no significant changes were seen in *HR*, *SV* and *CO*, but significant decreases in *MAP* were seen at the fifth visit during the study period. Systolic and diastolic pressures also tended to decrease during the study, but no statistical significance was reached. Thus, the cardio-protective effects of HRT (at least from the arterial stiffness perspective) seem to be limited to estrogen use alone.

5.2 Methodological Considerations and Limitations

Noninvasively recorded pressure waveforms are calibrated using blood pressures determined with an oscillometric sphygmomanometer at the brachial artery. This calibration procedure was based on two assumptions: mean and diastolic pressures are equal at all sites. Because viscous losses are minimal, mean pressure is assumed to be the

same at all sites, especially in healthy women with no obstructive vascular disease. It was reasonable to assume that diastolic pressures at different locations are relatively similar[56,58]. This issue of calibration was relevant only for the carotid pressure waveform because global mechanical property (e.g., Z_{in}, AC, SVR) calculations required these calibrated pressure values. However, PWV only required simultaneous waveform measurements; pressure calibration was not necessary.

The calculation of systemic arterial global mechanical properties requires simultaneous measurements of ascending aortic pressure and blood velocity (flow) waveforms. The carotid pressure waveform was used as a surrogate for the ascending aortic pressure waveform. These two waveform morphologies are reasonably similar, except for a slight time-delay in the carotid pressure waveform[54,56,60]. This time delay was corrected by aligning the carotid pressure upstroke with the rapid rise of the Doppler velocity signal.

Two assumptions were made to obtain volumetric flow from ascending aortic blood velocity measurements: a flat velocity profile in the radial direction and constant cross-sectional area or diameter (D_{LVOT}) over the cardiac cycle[61]. Although D_{LVOT} varies somewhat over the cardiac cycle, this change is quite small, especially at the aortic valve plane. There is experimental evidence for a flat velocity profile at the ascending aortic site[61,62].

The calculation of PWV requires the measurement of two quantities: the time delay between simultaneously measured pressure waveforms at two sites and the distance between these two sites. We had to identify the minimum (or foot) of the pressure waveform to obtain the time delay. This can be problematic because the noninvasively

recorded waveforms sometimes do not have a sharp minimum. To some extent, this problem is minimized by the intersecting tangent method used to identify the location of the pressure minimum[59]. Because blood velocity waveforms generally have a sharper upstroke, an alternative is to use simultaneously measured blood velocity waveforms at two sites to obtain the time delay. A typical pathway along the body surface was used to obtain the distance measurement between two sites. It is clear that potential measurement inaccuracies in this variable affect the absolute values of *PWV*. However, distances were measured only once for each subject (usually during the first visit) and this single set of values were used to calculate *PWV* at all times for a given subject. Thus, although the absolute *PWV* values may be questionable, the relative changes over time are valid.

The number of subjects in the HRT-all group is small (n=10), especially when one subdivides them into two groups (estrogen alone and estrogen + progesterone; n=5 in each group). Our inability to find statistically significant differences may be a result of the small number of subjects (i.e., low power). For example, although there was a clear trend for the carotid-to-femoral *PWV* to decrease, this did not reach statistical significance (Figure 19). Clearly, more subjects are necessary to address this issue.

5.3 General Hemodynamics

In general, *HR*, *S*V, and *CO* did not change significantly in either the control or HRT groups throughout the study period. West *el al*[63] have reported similar results in post-menopausal women receiving transdermal estradiol and oral progesterone for six months. However, Kamali *et al*[64] reported that *SV* and *CO* increased in perimenopausal

women receiving HRT (daily estradiol and intermittent norethindrone) after 5 weeks and these increases were maintained at 21 weeks. *MAP* decreased slightly over time in both control and HRT groups, reaching statistical significance at the fifth visit (Figure 11). However this decrease was small (~5%). Systolic and diastolic blood pressures tended to decrease over time as well, but these changes did not reach statistical significance (Figure 12 and 14). Other studies have reported essentially similar results regarding *MAP*[2,63] and systolic and diastolic blood pressures[65,66]. Overall, chronic HRT (HRT-E or HRT-EP) seems to have either no effects or only modest effects on general hemodynamic variables.

5.4 Systemic Vascular Global Mechanical Properties

Although Z_{in} is a comprehensive characterization of arterial mechanical properties, it is a relatively abstract quantification. No significant changes in Z_{in} were seen over time in the control group, while small decreases in the magnitude of Z_1 were seen in the HRT-E group, consistent with the possibility of increased global arterial compliance.

SVR did not change significantly over time in the control and HRT-E groups. Although a transient decrease in *SVR* was noted early on in the HRT-EP group, it returned to the baseline value at the end of the study (> 1 year). Similar early decrease in *SVR* with combined estrogen and progesterone treatment has also been reported by other studies[63,64,66].

AC was unchanged for the control subjects and tended to increase in the HRT-EP group, although this increase did not reach statistical significance. In contrast, *AC*

increased for the HRT-E group starting from the third visit and later reaching statistical significance at the fifth visit (Figure 18). Thus, it appears that the estrogen-mediated increase in vascular compliance (or reduction in stiffness) is a gradual process, requiring at least 3-6 months of treatment for a significant change. Although *AC* seems to increase in the HRT-EP group early on (e.g., at 200 days, Figure 18), the addition of progesterone completely abolishes the estrogen-mediated increase in *AC* at later stages (e.g., > 1 year, Figure 18). We could not find any previous studies examining HRT-induced changes in *AC* in post-menopausal women.

Chronic HRT did not affect global wave reflections as indicated by unchanged reflection index and magnitude of the first harmonic of reflection coefficient (Table 7-11). In contrast, we had previously observed reduced wave reflections during the third trimester of pregnancy wherein increased *AC* was accompanied by decreased *SVR*. Therefore, it is likely that changes in *SVR* may have a greater effect on global wave reflections than the effects of changes in *AC*.

Given that there were no significant changes in *CO* and *MAP* with chronic HRT, it is not surprising that the steady power was unchanged (Table 7-11). The observation that oscillatory power and percent oscillatory power did not change (Table 7-11) implies that chronic HRT did not have any adverse effects on ventricular-vascular arterial coupling from the perspective of energy wasted in pressure and flow pulsations.

5.5 Regional Vascular Mechanical Properties

Carotid-to-femoral ($PWV_{C\text{-}F}$) and brachial-to-radial ($PWV_{B\text{-}R}$) *PWV* were quantified in the present study as indices of regional vascular stiffness. The characterization of these two arterial segments allowed us to examine the effects of chronic HRT on larger central ($PWV_{C\text{-}F}$) and smaller peripheral ($PWV_{B\text{-}R}$) vessels.

$PWV_{C\text{-}F}$ increased over time for control subjects (Figure 19), an observation that is consistent with age-associated increase in vascular stiffness[16]. Although chronic HRT-E did not significantly change $PWV_{C\text{-}F}$ over time with respect to its own baseline value, there was a significant mitigation of the age-associated increase in $PWV_{C\text{-}F}$ seen in the control subjects, especially at Visits 2, 3, and 4 (Figure 19). Although this mitigation of age-associated increase in $PWV_{C\text{-}F}$ was also seen in the HRT-EP group, this effect was less pronounced during the early phases of the therapy (Visits 2 and 3, Figure 19). Scuteri *et al*[65] have reported identical findings with respect to the differential effects of HRT-E and HRT-EP on $PWV_{C\text{-}F}$. A decrease in $PWV_{C\text{-}F}$ in post-menopausal women on chronic HRT (some estrogen and some estrogen + progesterone) was also observed by Rajkumar *et al*[2]. However they did not provide data separated according to the type of HRT (estrogen vs. estrogen + progesterone).

$PWV_{B\text{-}R}$ did not change significantly over time for control subjects (Figure 20), indicating that the age-associated increase in vascular stiffness at the peripheral site is minimal over the observation period (~ 1 year). Chronic HRT-E significantly decreased brachial-to-radial stiffness as indicated by the decrease in $PWV_{B\text{-}R}$ (Figure 20). However, the inclusion of progesterone (HRT-EP group) completely eliminated the estrogen-

mediated decrease in brachial-to-radial arterial stiffness (Figure 20). In the same study by Rajkumar *et al*[2] mentioned above, a decrease in femoral-to-dorsal pedis artery *PWV* was observed; although this did not reach statistical significance. This failure of statistically significant decrease in peripheral vascular stiffness may be related to the mixing of different HRTs (estrogen and estrogen + progesterone) and/or the site of the peripheral arterial segment.

5.6 Mechanisms Underlying HRT-Induced Vascular Stiffness Changes

Global arterial compliance (*AC*) and pulse wave velocity (*PWV*) data were used to draw inferences regarding changes in vascular stiffness. Specifically, increased *AC* and/or decreased *PWV* were taken to imply reduced vascular stiffness and *vice a versa*. Potential mechanisms for increased *AC* and/or reduced *PWV* can be divided into three categories: (1) passive changes in vessels wall properties (stiffness) secondary to reduced distending pressure, (2) reduced smooth muscle tone, and (3) vascular wall remodeling.

The stress-strain relationship of the vessel wall material is typically nonlinear, resulting in distending pressure-dependent changes in vascular mechanical properties[67]. It is unlikely that this factor played a role in the present study for two reasons. First, *MAP* was reduced in both the control and HRT groups to the same extent. Second, the magnitude of this reduction was small (~ 5 mmHg for *MAP* and ~ 4 mmHg for aortic diastolic pressure). Based on the results of Carroll *et al*[58], this degree of reduction in distending pressure cannot totally account for the observed HRT-E-induced decrease in *PWV*.

It has been reported that acute administration of estrogen can cause vasodilation, mediated by the release of nitric oxide from vascular endothelial cells[42,43]. The release of nitric oxide reduces vascular smooth muscle tone[3]. In addition, Rajkumar *et al*[2] discussed the idea that vasodilation causes the transfer of vascular wall stress from the collagen fibers to the more distensible elastin fibers, allowing the vasculature to be more compliant. Thus, the reduction in smooth muscle tone may be the one of the mechanisms underlying the observed reductions in vascular stiffness with chronic HRT-E.

Regarding vascular remodeling (i.e., changes in vascular lumen and wall geometric properties and vessel wall composition), Westendorp *et al*[41] reported a slight increase in common carotid artery lumen diameter with chronic HRT (estrogen + progesterone). *In vitro* and animal studies have demonstrated that estrogen decreases collagen production and collagen/elastin ratio[68,69], decreases smooth muscle migration and proliferation[70,71], and accelerates endothelial cell growth[72,73]. Estrogen usage after menopause can also cause alterations in lipid profile: increases in high-density lipoproteins and decreases in low-density lipoproteins[35,74]. These changes in lipid profile are hopeful in decreasing the development of atherosclerosis and associated vascular wall remodeling. Thus, vascular remodeling may also play a role in HRT-E-induced reductions in vascular stiffness. However, data regarding chronic HRT-induced vascular geometric and compositional remodeling in the human setting are limited.

Age and physical training are known to affect *AC*[75]. There were no differences in age among the various groups. However, we do not have any information regarding physical fitness and activity of our study participants. Therefore, it is not possible to evaluate the potential confounding effects of this factor.

The main observation of the present study is that the inclusion of progesterone in HRT abolishes the estrogen-mediated decrease in vascular stiffness. Previous studies have shown chronic estrogen administration enhances endothelial-mediated vasodilation and progesterone inhibits this estrogen-mediated enhancement[76-79]. Although the exact mechanisms for the counteracting effects of progesterone are not clearly understood, possible causes may include downregulation of estrogen receptors and androgenic properties of progesterone (e.g., testosterone derivatives can exert vasoconstrictor influences, including decreases in prostacyclin). It should be noted that not all studies support the notion of progesterone-mediated counteracting effects on endothelial function[80,81].

5.7 HRT and Cardiovascular Risk

Earlier studies had suggested that chronic HRT is associated with certain cardio-protective effects. However, the most recent double blinded, randomized, placebo-controlled study (16,608 post-menopausal women with intact uterus) indicated that chronic HRT (estrogen + progesterone) was actually associated with an increased incidence of coronary heart disease, stroke, breast cancer, and pulmonary embolism[37]. A parallel study is examining the effects of chronic administration of estrogen alone in 10,739 women who have had a hysterectomy. At present, the balance of overall risks and benefits of estrogen-alone therapy remains uncertain. Our study indicates that the reduction in systemic arterial stiffness was limited to the estrogen alone group. If one accepts that increased vascular stiffness is an independent cardiovascular risk factor (see

Section 2.3) then estrogen alone therapy in post-menopausal women can conceivably be cardio-protective. However, given that estrogen is known to cause augmented cell proliferation leading to an increased incidence of endometrial carcinoma, estrogen alone therapy is limited to women who have had hysterectomy. It is possible that other estrogen preparations or alternative vasorelaxing agents may have the desirable effects on vascular stiffness properties without the risk of augmented cell proliferation. Further work is needed to examine this possibility.

5.8 Conclusions

The present study indicates chronic HRT in post-menopausal women is associated with reduced vascular stiffness (i.e., increased *AC* and reduced *PWV*) only when estrogen is used. Both reduced smooth muscle tone and vascular remodeling may be responsible for this estrogen-mediated decrease in vascular stiffness. The addition of progesterone seems to counteract the estrogen-mediated increase in *AC* and decrease in *PWV*, indicating that the vascular stiffness-associated cardio-protective effects of HRT, if any, may be limited to estrogen administration alone.

5.9 Future Directions

It would be worthwhile to investigate the exact mechanisms underlying the estrogen-mediated decrease in vascular stiffness and the counteracting effects of progesterone.

The present study indicates that there are regional differences in the estrogen-mediated vascular stiffness changes, with greater and more sustained responsiveness of smaller peripheral vessels (brachial-to-radial) than that of larger central vessels (carotid-to-femoral). Future studies should investigate the reasons for regional differences in responsiveness.

A search of estrogen alternative is also a worthwhile endeavor. It has been suggested that consumption of isoflavones (naturally occurring estrogen-like compounds) is associated with improved chronic disease burden[82]. For example, Japanese women have lower rates of cardiovascular disease than Western women. The soy isoflavones can stimulate estrogen receptors[83] and therefore, could be thought of as an alternative to traditional HRT.

Relaxin, an ovarian hormone, has been shown to have vasodilatory properties (e.g., renal vasodilation) via the nitric oxide pathway. Exogenous administration of relaxin to nonpregnant female rats (with or without ovaries) and male rats reproduces many of the hemodynamic features of pregnancy (increased cardiac output, renal flow, and glomerular filtration rate)[84,85]. Relaxin can also affect collagen degradation by upregulating the expression of matrix metalloproteinase[86]. These observations have led to the hypothesis that relaxin could favorably alter vascular stiffness, in a manner similar

to estrogen. It is worthwhile to investigate relaxin as a candidate to mediate the decline in systemic vascular resistance and concomitant rise in global arterial compliance.

APPENDIX

APPENDIX

Estimating Uncertainty in Calculated Variables Due to Measurement Inaccuracies

Systemic Vascular Resistance (SVR). Two measured variables are used to *SVR*: mean arterial pressure (*MAP*) and cardiac output (*CO*).

$$SVR = \frac{MAP}{CO}. \qquad (A1)$$

Thus, the total error in *SVR* (ΔSVR) due to measurement inaccuracies in *MAP* (ΔMAP) and *CO* (ΔCO) is given by:

$$\Delta SVR = \left|\frac{\partial SVR}{\partial MAP}\right| \left|\Delta MAP\right| + \left|\frac{\partial SVR}{\partial CO}\right| \left|\Delta CO\right|, \qquad (A2)$$

where $||$ denotes absolute value and $\frac{\partial SVR}{\partial MAP}$ and $\frac{\partial SVR}{\partial CO}$ represent partial derivatives of *SVR*, given by (from *Equation A1*):

$$\frac{\partial SVR}{\partial MAP} = \frac{1}{CO} \qquad (A3)$$

$$\frac{\partial SVR}{\partial CO} = -\frac{MAP}{CO^2}. \qquad (A4)$$

Given nominal values of *MAP* and *CO* and uncertainties in measured variables (ΔMAP and ΔCO), one can calculate ΔSVR using *Equations A2-A4*. Percentage error can now be calculated by dividing ΔSVR by the nominal value of *SVR*.

Global Arterial Compliance (AC). The equation for the estimation for *AC* from the diastolic aortic pressure decay method is (same as *Equation 3-1*):

$$AC = \frac{A_d}{SVR(P_1 - P_2)} \qquad (A5)$$

We need to write this equation in terms of measured quantities: *MAP*, *CO*, P_d (arterial diastolic pressure), and t_d (duration of diastole). P_1, aortic pressure at the end of ejection (Figure 7), is assumed to equal *MAP*[87], P_2 is the same as P_d, and *SVR* = *MAP*/*CO*. In order to express A_d (area under the diastolic portion, Figure 7, as a function of measured variables, we have to assign an explicit functional form to the pressure waveform: *P(t)* $= P(t) = P_0 * e^{-\frac{t}{\tau}}$. We will also assume that this equation exactly passes through *MAP* (at t = 0) and P_d (at $t = t_d$) so that we can write P_0 and τ (and consequently, A_d) in terms of measured quantities. With these considerations, *Equation A4* can be rewritten in terms of measured quantities as follows:

$$AC = \frac{CO}{MAP} \frac{t_d}{\ln\left(MAP / P_d\right)} \qquad (A6)$$

Thus, the total error in *AC* (ΔAC) due to measurement inaccuracies can be written as:

$$\Delta AC = \left|\frac{\partial AC}{\partial CO}\right| \left|\Delta CO\right| + \left|\frac{\partial AC}{\partial t_d}\right| \left|\Delta t_d\right| + \left|\frac{\partial AC}{\partial MAP}\right| \left|\Delta MAP + \left|\frac{\partial AC}{\partial P_d}\right| \left|\Delta P_d\right|\right|, \qquad (A7)$$

where the partial derivatives are given by:

$$\frac{\partial AC}{\partial CO} = \frac{t_d}{MAP \times \ln\left(MAP / P_d\right)} \qquad (A8)$$

$$\frac{\partial AC}{\partial t_d} = \frac{CO}{MAP \times \ln\left(MAP / P_d\right)} \qquad (A9)$$

$$\frac{\partial AC}{\partial P_d} = \frac{CO}{MAP \times P_d} \frac{t_d}{\ln\left(MAP/P_d\right)^2} \qquad (A10)$$

$$\frac{\partial AC}{\partial MAP} = \frac{CO}{MAP} \frac{t_d}{MAP \times \ln\left(MAP/P_d\right)^2} - \frac{CO}{MAP^2} \frac{t_d}{MAP \times \ln\left(MAP/P_d\right)}. \qquad (A11)$$

Given nominal values of *MAP*, *CO*, P_d, and t_d and uncertainties in measured variables (ΔMAP, ΔCO, ΔP_d, and Δt_d), one can calculate ΔAC using *Equations A7-A11*. Percentage error can now be calculated by dividing ΔAC by the nominal value of *AC*.

Table 17: Uncertainty in Calculated Variables Due to Measurement Inaccuracies

	Nominal Value	Error
Measured Variables		
CO (ml/s)	85[a]	1.0 (ref. 88)
t_d (s)	0.6[a]	.0025[b]
P_d (mmHg)	65[a]	1.5 (ref. 89)
MAP (mmHg)	90[a]	1.5[d]
Calculated Variables		
SVR (dyne.s/cm^5)	1411	40 (2.8%)
AC (mL/mmHg)	1.74	0.27 (15.5%)

[a] Present study (Table 2); [b] Sampling rate in the present study.

We believe that the calculated percentage error for *AC* is an overestimation for two reasons. First, in order to represent A_d in terms of measured quantities (*MAP*, *CO*, P_d, and t_d), we had to assume an explicit functional form (exponential) for the diastolic pressure decay and force this function to pass through the two end points (*MAP* and P_d). This results in unduly large errors in A_d for given measurement errors in *MAP* and P_d. Second, an experimental study[90] indicated that *AC* values derived using noninvasive techniques (similar to those in the present study) were similar to those derived using invasive pressure and flow data (most of the values were within 10% of each other).

BIBLIOGRAPHY

BIBLIOGRAPHY

1. Izzo JL, Shykoff BE. Arterial Stiffness: Clinical relevance, measurement, and treatment. *Rev Cardiol Med* 2(1):29-40, 2001.

2. Rajkumar C, Kingwell BA, Cameron JD, *et al*. Hormonal therapy increases arterial compliance in postmenopausal women. *J Am Coll Cardiol* 30:350-6, 1997.

3. Mendelsohn ME, Karas RH. The protective effects of estrogen on the cardiovascular system. *The N Eng J Med* 340:1801-1811, 1999.

4. Samaan SA, Crawford MH. Estrogen and cardiovascular function after menopause. *J Am Coll Cardiol* 26:1403-1410, 1995.

5. Reis SE, Holubkov R, Young JB, White BG, Cohn JN, Feldman AM. Estrogen is associated with improved survival in aging women with congestive heart failure: analysis of the Vesnarinone studies. *J Am Coll Cardiol* 36:529-33, 2000.

6. Vander A, Sherman J, Luciano D. Circulation. In: *Human physiology: The mechanisms of body function 7th ed*. WCB Mcgraw-Hill, 1998, 372-460.

7. Milnor WR. Arterial impedance as ventricular afterload. *Circ Res* 36:565-570, 1975.

8. Nichols WW, Pepine CJ, Geiser EA, Conti CR. Vascular load defined by the aortic input impedance spectrum. *Federation Proc* 39:196-201, 1980.

9. O'Rourke MF, Taylor MG. Input impedance of the systemic circulation. *Circ Res* 20:365-380, 1967.

10. O'Rourke MF. Vascular impedance in studies of arterial and cardiac function. *Physiol Rev* 62:570-623, 1982.

11. Nichols WW and O'Rourke MF. *McDonald's Blood Flow in Arteries*. Edward Arnold, London, 3rd ed. 1990.

12. Milnor WR. *Hemodynamics*. Williams & Wilkins, Baltimore, 1989

13. Asmar R. *Arterial stiffness and pulse wave velocity*. Elsevier SAS, 1999.

14. Liu Z, Brin KP, Yin FCP. Estimation of total arterial compliance: an improved method and evaluation of current methods. *Am J Physiol* 251:H588-H600, 1986.

15. Toorop GP, Westerhof N, Elzinga G. Beat-to-beat estimation of peripheral resistance and arterial compliance during pressure transients. *Am J Physiol* 252:H1275-H1283, 1987.

16. London GM, Marchais SJ, Safar ME, Genest AF, Guerin AP, Metivier F, Chedid K, London AM. Aortic and large artery compliance in end-stage renal failure. *Kidney Int* 37(1):137-42, 1990.

17. Bortolotto LA, Blacher J, Kondo T, Takazawa K, Safar ME. Assessment of vascular aging and atherosclerosis in hypertensive subjects: Second derivative of photoplethysmogram versus pulse wave velocity. *AJH* 13:165-171, 2000.

18. Westerhof N, Sipkema P, Van den Bos GC, Elzinga G. Forward and backward waves in the arterial system. *Cardiovasc Res* 6:648-656, 1972.

19. Noordergraaf A. *Circulatory System Dynamics*. Academic Press, New York, 1978.

20. Wemple RR, Mockros LF. Pressure and flow in the systemic arterial system. *J Biomech* 5:629-641, 1972.

21. Berger DS, Li JK-J, Noordergraaf A. Differential effects of wave reflections and peripheral resistance on aortic blood pressure: a model based study. *Am J Physiol* 266:H1626-H1642, 1994.

22. Messerli FH. *The Heart and Hypertension*. Yorke Medical, New York, 1987.

23. Devereux RB, de Simone G, Ganau A, Roman MJ. Left ventricular hypertrophy and geometric remodeling in hypertension: stimuli, functional consequences and prognostic implications. *J Hypertens* 12:S117-S127, 1994.

24. O'Rourke MF. Basic concepts for the understanding of large arteries in hypertension. *J Cardio Pharm* 7:S-14-S-21, 1985.

25. Sandor B. *Fundamentals of Cyclic Stress and Strain*. University of Wisconsin, Madison, 1972.

26. Kannel WB, Gordon T, Schwartz MJ. Systolic versus diastolic blood pressure and risk of coronary heart disease. *Am J Cardiol* 27:335, 1970.

27. Kannel WB, Dawber TR, McGee DL. Perspectives on systolic hypertension: the Framingham study. *Circulation* 61:1179-1182, 1980.

28. Kannel WB, Wolf PA, McGee DL, Dawber TR, McNamara P, Castelli WP. Systolic blood pressure, arterial rigidity, and risk of stroke. *JAMA* 245:1225-1229, 1981.

29. Curb JD, Borhani NO, Entwisle G, Tung B, Kass E, Schnaper H, Williams W, Berman R. Isolated systolic hypertension in 14 communities. *Am J Epidemiol* 121:362-370, 1985.

30. Johnson JL, Heineman EF, Heiss G, Hames CG, Tyroler HA. Cardiovascular disease risk factors and mortality among black women and white women aged 40-64 years in Evans County, Georgia. *Am J Epidemiol* 123:209-220, 1986.

31. Tverdal A. Systolic and diastolic blood pressure as predictor of coronary heart disease in midde-aged Norwegian men. *Br Med J* 294:671-673, 1987.

32. Hagman M, Wilhelmsen L, Wedel H, Pennert K. Risk factors for angina pectoris in a population study of Swedish men. *J Chron Dis* 40:265-275, 1987.

33. Darne B, Girerd X, Safar M, Cambien F, Guize L. Pulsatile versus steady component of blood pressure: a cross-sectional analysis and a prospective analysis on cardiovascular mortality. *Hypertension* 13:392-400, 1989.

34. Rajkumar C, Kingwell BA, Cameron JD, Waddell T, Mehra R, Christophidis N, Komesaroff PA, McGrath B, Jennings GL, Sudhir K, Dart AM. Hormonal therapy increases arterial compliance in postmenopausal women. *Atherosclerosis* 30(2):350-6, 1997.

35. Samaan SA, Crawford MH. Estrogen and cardiovascular function after menopause. *J Am Coll Cardiol* 26:1403-1410, 1995.

36. Grady D, Herrington D, Bittner V, Blumenthal R, Davidson M, Hlatky M, Hsia J *et al*. Cardiovascular disease outcomes during 6.8 years of hormone therapy: Heart and estrogen/progestin replacement study follow-up (HERS II). *JAMA* 288(2):49-57, 2002.

37. Writing group for the women's health initiative investigators. Risks and benefits of estrogen plus progestin in healthy postmenopausal women: Principal results from the women's health initiative randomized controlled trial. *JAMA* 288(3), 2002.

38. Hallock P. Arterial elasticity in man in relation to age as evaluated by the pulse wave velocity method. *Arch Int Med* 54:770-98, 1934.

39. Avolio AP, Fa-Quan D, Wei-Quang L, Yao-Fei L, Zhen-Dong H, Lian-Fen X, *et al*. Effects of aging on arterial distensibility in populations with high and low prevalence of hypertension: comparison between urban and rural communities in China. *Circulation* 71:202-10, 1985.

40. Avolio AP. Pulse wave velocity and hypertension. In: Safa ME, ed. Arterial and venous systems in essential hypertension. Martinus Nijhoff. P.133-52, 1987.

41. Westendorp ICD, Kleijn MJJ, Bots ML, Bak AAA, Planellas J, Coelingh Bennink HJT, Hofman A, Grobbee DE, Witteman JCM. The effect of hormone replacement therapy on arterial distensibility and compliance in perimenopausal women: a 2-year randomized trial. *Atherosclerosis* 152:149-159, 2000.

42. Chen Z, Yuhanna IS, Galcheva-Gargova Z, Karas RH, Mendelsohn ME, *et al*. Estrogen receptor alpha mediates nongenomic activation of eNOS by estrogen. *J Clin Invest* 103:401-6, 1999.

43. Mendelsohn ME, Karas RH. The protective effects of estrogen on the cardiovascular system. *N Engl J Med* 340:1801-11, 1999.

44. Tsiamis E, Stefanadis C, Stratos C, *et al*. The effect of estrogen on the elastic properties of the aorta in post-menopausal women [abstract]. *Circulation* 92 Suppl I:I-2615, 1995.

45. Fischer GM. In vivo effects of estradiol on collagen and elastin dynamics in rat aorta. *Endocrinology* 91:1227-1232, 1972.

46. Dai-Do D, Espinosa E, Liu G, *et al*. 17β-estradiol inhibits proliferation and migration of human vascular smooth muscle cells: similar effects in cells from postmenopausal females and males. *Cardiovasc Res* 32:980-985, 1996.

47. Lehmann ED, Hopkins KD, Parker JR, Turay RC, Rymer J, Fogelman I, Gosling RG. Aortic Distensibility in post-menopausal women receiving Tibolone. *Br J Radiol* 67(799):701-5, 1994.

48. Lin AL, Shain SA. Estrogen-mediated cytoplasmic and nuclear distribution of rat cardiovascular estrogen receptors. *Arteriosclerosis* 5(6):668-77, 1985.

49. Losordo DW, Kearney M, Kim EA, Jekanowski J, Isner JM. Variable expression of the estrogen receptor in normal and atherosclerotic coronary arteries of premenopausal women. *Circulation* 89(4):1501-10 1994.

50. Manolio TA, Furberg CD, Shemanski L, Psaty BM, O'Leary DH, Tracy RP, Bush TL. Associations of postmenopausal estrogen use with cardiovascular disease and its risks factors in older women. The CHS Collaborative Research Group. *Circulation* 88(5 Pt 1):2163-71, 1993.

51. Kelly R, Hayward C, Ganis J, Daley J, Avolio A, O'Rourke M. Noninvasive registration of the arterial pressure pulse waveform using high-fidelity applanation tonometry. *J Vasc Med Biol* 1:142-149, 1989.

52. Sato T, Nishinaga M, Kawamoto A, Ozawa T, Takatsuji H. Accuracy of a continuous blood pressure monitor based on arterial tonometry. *Hypertension* 21:866-874, 1993.

53. Drzewiecki GM, Melbin J, Noordergraaf A. Arterial tonometry: review and analysis. *J Biomech* 16:141-153, 1983.

54. Kelly R, Karamanoglu M, Gibbs H, Avolio A, O'Rourke M. Non-invasive carotid pressure wave registration as an indicator of ascending aortic pressure. *J Vasc Med Biol* 1:241-247, 1989.

55. Saba PS, Roman MJ, Pini R, Spitzer M, Ganau A, Devereux RB. Relation of arterial pressure waveform to left ventricular and carotid anatomy in normotensive subjects. *J Am Coll Cardiol* 22:1873-1880, 1993.

56. Kelly R, Fitchett D. Noninvasive determination of aortic input impedance and external left ventricular power output: a validation and repeatability study of a new technique. *J Am Coll Cardiol* 20:952-963, 1992.

57. Guerin AP, Pannier BM, Marchais SJ, Metivier F, Safar M, London GM. Effects of antihypertensive agents on carotid pulse contour in humans. *J Human Hypertens* 6:S-37-S-40, 1992.

58. Carroll JD, Shroff S, Wirth P, Halsted M, Rajfer SI. Arterial mechanical properties in dilated cardiomyopathy. *J Clin Invest* 87:1002-1009, 1991.

59. Chiu YC, Arand PW, Shroff SG, Feldman T, Carroll JD. Determination of pulse wave velocities with computerized algorithms. *Am Heart J* 121:1460-1470, 1991.

60. Marcus RH, Korcarz C, McRay G, Neumann A, Murphy M, Borow K, Weinert L, Bednarz J, Gretler DD, Spencer KT, Sareli P, Lang RM. Noninvasive method for determination of arterial compliance using echocardiography and subclavian pulse tracings: validation and clinical application of a physiological model of circulation. *Circulation* 89:2688-2699, 1994.

61. Gill RW. Measurement of blood flow by ultrasound: accuracy and sources of error. *Ultrasound Med Biol* 11:625-41, 1985.

62. Fisher DC, Sahn DJ, Friedman MJ, Larson D, Valdes-Cruz LM, Horowitz S, Goldberg SJ, Allen HD. The mitral valve orifice method for noninvasive two-dimensional echo Doppler determinations of cardiac output. *Circulation* 67:872-7, 1983.

63. West SG, Hinderliter AL, Wells EC, Girdler SS, Light KC. Transdermal estrogen reduces vascular resistance and serum cholesterol in postmenopausal women. *Am J Obstet Gynecol* 184:926-33, 2001.

64. Kamali P, Muller T, Lang U, Clapp JF 3rd. Cardiovascular responses of perimenopausal women to hormonal replacement therapy. *Am J Obstet Gynecol* 182(1 Pt 1):17-22, 2000.

65. Scuteri A, Lakatta EG, Bos AJ, Fleg JL. Effect of estrogen and progestin replacement on arterial stiffness indices in postmenopausal women. *Aging (Milano)* 13(2):122-30, 2001.

66. Light KC, Hinderliter AL, West SG, Grewen KM, Steege JF, Sherwood A, Girdler SS. Hormone replacement improves hemodynamic profile and left ventricular geometry in hypertensive and normotensive postmenopausal women. *J Hyper* 19:269-278, 2001.

67. Nichols WW, O'Rourke MF. McDonald's blood flow in arteries, theoretical, experimental, and clinical principles. London: Edward Arnold, 398-420, 1990.

68. Riedel M, Rafflebeul W, Lichtlen P. Ovarian sex steroids and atherosclerosis. *Clin Invest* 71:406:412, 1993.

69. Beldekas JC, Smith B, Gerstenfeld LC, Sonenshein GE, Franzblau C. Effects of 17 beta-estradiol on the biosynthesis of collagen in cultured bovine aortic smooth muscle cells. *Biochemistry* 20:2162-2167, 1981.

70. Kolodgie FD, Jacob A, Wilson PS, et al. Estradiol attenuates directed migration of vascular smooth muscle cells *in vitro*. *Am J Pathol* 148:969-76, 1996.'

71. Bhalla RC, Toth KF, Bhatty RA, Thompson LP, Sharma RV. Estrogen reduces proliferation and agonist-induced calcium increase in coronary artery smooth muscle cells. *Am J Physiol* 272:H1996-H2003, 1997.

72. Morales DE, McGowan KA, Grant DS, et al. Estrogen promotes angiogenic activity in human umbilical vein endothelial cells *in vitro* and in a murine model. *Circulation* 95:1768-72, 1997.

73. Krasinski K, Spyridopoulos I, Asahara T, van der Zee R, Isner JM, Losordo DW. Estrogen accelerates functional endothelial recovery after arterial injury. *Circulation* 95:1768-72, 1997.

74. Wild RA. Estrogen: Effects on the cardiovascular tree. *Obstet Gynecol* 87:27S-35S, 1996.

75. Cameron JD, Dart AM. Exercise training increases total systemic arterial compliance in humans. *Am J Physiol* 266:H693-701, 1994.

76. Adams MR, Register RC, Golden DL, *et al*. Medroxyprogesterone acetate antagonizes inhibitory effects of conjugated equine estrogens on coronary artery atherosclerosis. *Arterioscler Thromb Vasc Biol* 17:217-221, 1997.

77. Miyagawa K, Rosch J, Stanczyk F, *et al*. Medroxyprogesterone interferes with ovarian steroid protection against coronary vasospasm. *Nat Med* 3:324-327, 1997.

78. Williams JK, Delansorne R, Paris J. Estrogens, progestins, and coronary artery reactivity in atherosclerotic monkeys. *J Steroid Biochem Mol Biol* 65:219-24, 1998.

79. Wakatskui A, Okatani Y, Ikenoue N, Fukaya T. Effect of medroxyprogesterone acetate on endothelium-dependent vasodilation in postmenopausal women receiving estrogen. *Circulation* 104:1773-1778, 2001.

80. Dinh H, Nathan L. Medroxyprogesterone acetate does not antagonize estrogen-induced increases in endothelium-dependent vasodilation: potential clinical implications. *Fertility and sterility* 78(1):122-127, 2002.

81. Campisi R, Nathan L, Pampaloni MH, Schoder H, Sayre JW, Chaudhuri G, Schelbert HR. Noninvasive assessment of coronary microcirculatory function in postmenopausal women and effects of short-term and long-term estrogen administration. *Circulation* 105:425-430, 2002.

82. Thom TJ, Epstein FH, Feldman JJ, Leaverton PE, Wolz M. Total morbidity and mortality from heart disease, cancer and stroke from 1950 to 1987in 27 countries. National Institutes of Health Publication No.92-3088, MD.

83. Kuiper GG, Lemmen JG, Carlsson B, Corton JC, Safe SH, Van der Saag PT *et al*. Interaction of estrogenic chemicals and phytoestrogens with estrogen receptor beta. *Endocrinology* 138:4252-4263, 1998.

84. Danielson LA, Sherwood OD, Conrad KP. Relaxin is a potent renal vasodilator in conscious rats. *J Clin Invest* 103:525-533, 1999.

85. Danielson LA, Kerchner LJ, Conrad KP. Impact of gender and endothelin on renal vasodilation and hyperfiltration induced by relaxin in conscious rats. *Am J Physiol* 279(4):R1298-304, 2000.

86. Unemori EN, Pickfor LB, Salles AL, Piercy CE, Grove BH, Erikson ME, Amento EP. Relaxin induces an extracellular matrix-degrading phenotype in human lung fibroblasts in vitro and inhibits lung fibrosis in a murine model in vivo. *J Clin Invest* 98:2739-2745, 1996.

87. Sunagawa K, Maughan WL, Burkhoff D, Sagawa K. Left ventricular interaction with arterial load studied in isolated canine ventricle. *Am J Phyiol* H773-H780, 1983.

88. Spencer KT, Lang RM, Neumann A, Borow KM, Shroff SG. Doppler and electromagnetic comparisons of instantaneous aortic flow characteristics in primates. *Circ Res* 68:1369-1377, 1991.

89. Zorn EA, Wilson MB, Angel JJ, Zanella J, Alpert BS. Validation of an automated arterial tonometry monitor using association for the advancement of medical instrumentation standards. *Blood Pressure Monitoring* 2:185-188, 1997.

90. Marcus RH, Korcarz C, McCray G, Neumann A, Murphy M *et al*. Noninvasive method for determination of arterial compliance using Doppler echocardiography and subclavian pulse tracings, validation and clinical application of a physiological model of the circulation. *Circulation* 89:2688-2699, 1994.